CHARACTERIZATION OF TWO-COMPONENT ORGANOTHIOL MIXED MONOLAYERS ON GOLD AND QUANTIFICATION OF NONSPECIFIC ADSORPTION ON MIXED SAM BIOSENSOR PLATFORMS USING ELECTROCHEMICAL ENZYME IMMUNOASSAY

Except where reference is made to the work of others, the work described in this thesis is my own or was done in collaboration with my advisory committee. This thesis does not include proprietary or classified information.

_____

Huiqing Liu

Certificate of Approval:

_____	_____
Vince Cammarata Associate Professor Chemistry & Biochemistry	Curtis G. Shannon, Chair Professor Chemistry & Biochemistry
_____	_____
Wei Zhan Assistant Professor Chemistry & Biochemistry	George T. Flowers Interim Dean Graduate School

CHARACTERIZATION OF TWO-COMPONENT ORGANOTHIOL MIXED MONOLAYERS ON GOLD AND QUANTIFICATION OF NONSPECIFIC ADSORPTION ON MIXED SAM BIOSENSOR PLATFORMS USING ELECTROCHEMICAL ENZYME IMMUNOASSAY

Huiqing Liu

A Thesis

Submitted to

the Graduate Faculty of

Auburn University

in Partial Fulfillment of the

Requirements for the

Degree of

Master of Science

Auburn, Alabama
May 10, 2007

CHARACTERIZATION OF TWO-COMPONENT ORGANOTHIOL MIXED MONOLAYERS ON GOLD AND QUANTIFICATION OF NONSPECIFIC ADSORPTION ON MIXED SAM BIOSENSOR PLATFORMS USING ELECTROCHEMICAL ENZYME IMMUNOASSAY

Huiqing Liu

_____
Signature of Author

_____
Date of Graduation

VITA

Huiqing Liu, daughter of Zhenshou Liu and Yazhen Zhou, was born February 1, 1978, in Jianou City, Fujian Province, People's Republic of China. She graduated from the First High School of Jianou in 1996 and went on to attend Donghua University, People's Republic of China, in September, 1996, graduating with a Bachelor of Applied Chemistry degree in Chemical Engineering in 2000. She then worked as a chemical engineer at the Shanghai Chemical Plant Company of China for several years. In August 2004, she began her graduate studies in the Department of Chemistry and Biochemistry at Auburn University.

THESIS ABSTRACT

CHARACTERIZATION OF TWO-COMPONENT ORGANOTHIOL MIXED MONOLAYERS ON GOLD AND QUANTIFICATION OF NONSPECIFIC ADSORPTION ON MIXED SAM BIOSENSOR PLATFORMS USING ELECTROCHEMICAL ENZYME IMMUNOASSAY

Huiqing Liu

Master of Science, May 10, 2007
(B.S., Donghua University, P. R. China, 2000)
108 Typed pages

Directed by Curtis G. Shannon

Self-assembled monolayer (SAM) technology provides a simple and useful way to functionalize biosensors. The formation and characterization of SAM monolayers are briefly reviewed in Chapter One. Several selected examples of SAM based biosensors were introduced. Because the sensitivity of a biosensor depends on its nonspecific adsorption of immumoactive organisms, a brief introduction to the principles and methods to inhibit nonspecific adsorption on biosensors is also given in Chapter One.

In Chapter Two, the theory governing the formation of two-component SAMs is discussed. The mechanism controlling the final composition of the mixed monolayer can

either be kinetically or thermodynamically controled. Two-component SAMs containing alkanethiol/ olig(ethylene glycol) (OEG) thiol, 4-aminothiophenol/alkanethiol and 4-aminothiophenol/olig(ethylene glycol) thiol were characterized using capacitance and coulometry measurements and surface-enhanced Raman spectroscopy. The adsorption isotherms for these mixed SAMs systems were discussed by the model of thermodynamic control in the formation of mixed monolayer.

Nonspecific adsorption of immunoactive molecules on a biosensor's surface is an important way to minimize of nonspecific adsorption on SAM-based biosensor platforms is discussed in Chapter Three. Protein adsorption on mixed SAMs of decanethiol (DT) and tetraethylene glycol thiol (EG_4-SH) was quantified using electrochemical enzyme immunoassay. The protein adsorption is reduced more on the OEG-SAM surface than on hydrophobic decanethiol SAM surface. Both thiols were used as blocking agents in immuno-sandwich biosensor platforms with mixed SAMs to confirm that an EG_4-SH monolayer inhibits of nonspecific adsorption better than a DT monolayer.

Chapter Four provides general conclusions on the characterization of two-component organothiol mixed monolayers on gold and quantification of nonspecific adsorption on mixed SAMs biosensor platforms using an electrochemical enzyme immunoassay**.**

ACKNOWLEDGMENTS

The author would like to thank her research advisor, Dr. Curtis Shannon for his guidance and assistance throughout her graduate studies. Thanks are extended to Dr. Vince Cammarata and Dr. Wei Zhan for their suggestions and for serving as advisory committee members. The author appreciates all the faculty and staff in the chemistry department and members of Dr. Shannon research group for their assistance during her graduate studies at Auburn University.

The author would also like to thank her family, especially her husband, for their encouragement and support throughout the duration of her studies. Finally, thanks are due to the many friends who shared in the graduate school experience.

Style manual or journal used Journal of the American Chemical Society

Computer software used Microsoft Office XP, EndNote6.0, OriginPro 7.5

TABLE OF CONTENTS

LIST OF TABLES

LIST OF SCHEMES

LIST OF FIGURES

CHAPTER 1

INTRODUCTION TO SELF-ASSEMBLED MONOLAYER-BASED BIOSENSORS AND RESISTANCE TO NONSPECIFIC ADSORPTION ON BIOSENSORS

1.1 Introduction

Immunoassays have many important applications in fields such as food processing, clinical diagnostics, environmental monitoring and control, pubic safety and the pharmaceutical industry. Consequently, research on new biosensors and the further development of currently available biosensors has increased tremendously over the past decade. A biosensor is a compact analytical device incorporating a biological recognition system that is either integrated within or intimately associated with a physicochemical transducer.[1] The molecular specific sensing elements on the biological recognition system surface can capture picomolar concentrations of specific analytes from a biological sample. An electrochemical, optical or piezoelectric transducer is then used to convert the interaction between the sensing elements and analytes into a measurable chemical or physical output signal, whose magnitude is related to the concentration or amount of analyte present in the biological sample. Numerous studies of biomolecular interactions have been reported, including receptor cell recognition of species attached to various types of surfaces. Most commonly, the molecular specific

sensing elements are immobilized on the surface of transducer. There are many ways to immobilize the sensing species on a sensor surface. For example, direct immobilization of biomolecules can be achieved by physical adsorption on solid surfaces or by the formation of artificial (synthetic) receptor layers. However, direct immobiliztion of biomolecules, results in the biomolecules being adsorbed with various orientations, unfolding often occurs and the layer created suffers from poor stability. Compared to biological molecules, artificial layers have better stability while still retaining good specificity. The self-assembled monolayer is one of the artificial layers used for designing molecule specific surfaces.

Self-assembled monolayers (SAMs) are highly ordered chemisorbed organic single layers formed by spontaneous adsorption of an active surfactant onto a solid surface. Self-assembled monolayer technology provides a very useful and powerful tool to generate mono-molecular films of biological molecules on a variety of surfaces, This technique has developed dramatically in terms of its synthetic sophistication and depth of characterization over the last two decades and is now applied for the development of various detectors. Since SAMs have the flexibility to be modified easily at the single molecular level, the modification of solid substrates by self-assembling monolayers is a very useful research model system that is used to promote the self-organization mechanism of molecules, molecular structure and property relationships and phenomena at the interface between different phases.

Biosensors have some strict requirements, such as the size of the device, the selective response of the analyte, and the need for a fast response time. Biological scientists are therefore continually searching for some new and improved materials to overcome some

or all of these limitations. Self-assembled monolayers provide several attractive features for these applications. First, miniaturization is easy due to the minimal resources needed (e.g. a monolayer may contain as few as 10^{13} molecules/cm^2 or only 10^{-7} moles/cm^2). Secondly, the very simple procedure used for SAM formation and its compatibility with solid substrates for electrochemical measurements offer special benefits for biosensor applications involving current or potential measurements. Thirdly, the highly ordered and dense nature of the long chain self-assembled alkanethiol monolayers mimics the cellular microenvironment of lipid bilayer structures, thus offering novel substrates for immobilized biomolecules or biological systems. Finally, the chemical stability of a monolayer results in a transducer that is integrated with a biological recognition system for use in immunosensors and biosensors, even after the SAM has been combined with the immobilizing molecules as a result of their associated specificity and molecular recognition.

1.2 Self-assembled monolayers

There are several methods that can be used to prepare organic ultra-thin films. For thin polymer films, sputtering coating is the most popular preparation method[4]. For crystalline films composed of relatively small molecules, there are several common routes. For example, Langmuir films consist of amphiphilic molecules dispersed on a liquid surface like water,[5] where the hydrophilic head group has an affinity to the water while the hydrophobic end group sticks up away from the water. The Langmuir-Blodgett technique involves the transfer of a film, preassembled at an air-water interface, onto a solid surface.[6] Organic molecular beam deposition (OMBD) or organic molecular beam

epitaxy (OMBE) which is very similar to evaporation techniques in ultrahigh vacuum (UHV), has also been used for inorganic materials [7-9]and self assembly. Compared to these techniques for the preparation of organic thin film, SAMs rely on an easy and near-equilibrium procedure and have a strong chemisorption between adsorbate and substrate. Many systems can undergo the process of self-assembly: long-chain n-alkanoic acid ($C_nH_{2n+1}COOH$) at metal oxide substrates[10-12]; organosilane species ($RSiX_3$, R_2SiX_2 or R_3SiX, where R is an alkyl chain and X is a chloro or alkoxy group) at hydroxylated substrates, such as silicon oxide[13-18], glass[18], mica[19-21] and aluminum oxide[22,23]; and organosulfur adsorbates on metal and semiconductor surfaces[24-27]. Biological scientists are particularly interested in the latter system as it is the best characterized in terms of stability and the physicochemical properties of the organosulfur-based species.

1.2.1 Formation of monolayers

Self-assembled monolayer formation is induced by the strong chemical interactions between the surface and the head group of the selected organic molecule. Surface-active organosulfur compounds have a strong affinity to transition metal surfaces. Organosulfur-based species include di-*n*-alkyl sulfide[28,29], di-*n*-alkyl disulfides[30], thiophenols[31,32], mercaptopyridines[32], mercaptoanilines[33], thiophenes[34], cysteines[35,36], xanthates[37], thiocarbaminates[38], thiocarbamates[39], thioureas[40], mercaptoimidazoles[41-43], and alkaneselenols[44]. However, the most interesting, well-studied and best understood SAM is alkanethiol adsorbed on a gold substrate, which will therefore be the focus of the following discussion. This is a very simple way to prepare SAM monolayers. The clean substrate is immersed into the required dilute solution for a specified time, followed by

thorough washing with the same solvent and drying with dry nitrogen or argon gas. The monolayers formed from alkanethiols and dialkyl disulfide are indistinguishable[45], resulting in the same thiolate species on a clean gold surface. In the case of disulfides, the mechanism of bonding is considered to be a simple oxidative addition of the S-S bond to the gold surface.

$$RS{-}SR + Au_n^0 \Rightarrow RS^-Au^+ \cdot Au_{n-1}^0$$

The mechanism for the formation of SAM from alkanethiol is thought to be an oxidative addition of the S-H bond to the gold surface, followed by a reductive elimination of the hydrogen, and the formation of a thiolate species[6,46]. When a clean gold surface is used, the eliminated hydrogen can combine to form an H_2 molecule.

$$R{-}S{-}H + Au_n^0 \Rightarrow R{-}S^-Au^+ \cdot Au_{n-1}^0 + {}^1/_2H_2$$

To understand and control the formation of self-assembled monolayers, a great deal of research has been carried out on the kinetics of SAM formation. There are two distinct adsorption processes which occur in the formation of SAMs[46,47]: the first process consists of the sulfur-based compound assembling on the metal surface, which is a very fast step, taking only a few minutes by the end of which the contact angles are close to their limiting values and the thickness has reached about 80%-90% of its maximum value. The second process is a slow one that may last several hours where the alkyl chains rearrange by undergoing van der Waals interaction between neighboring hydrocarbon chains to generate an extended close packed, all-trans conformation [48-50]. The kinetics of the second process is related to alkyl chain disordering such as gauche defects, the

chain-chain interactions such as van der Waals forces and dipole-dipole interactions between neighboring individual molecules, and the surface mobility of chains.

The orientation, structure and packing density of alkanethiolate momolayers are affected by several factors, such as the choice of solvent[51], the nature and concentration of the adsorbate[47], the temperature, the soaking time and the surface properties of the metal substrates[52]. Thiols, sulfides or disulfides can be easily adsorbed onto the surface from high purity solvents, such as ethanol, water, hexane, or acetonitrile. Smoother and cleaner surfaces, often metallic, produce more densely packed and well-ordered molecular monolayers than rougher surfaces. The attractive van der Waal forces between the alkyl chains enhance the order, so the level of defects and stability of the SAMs, the degrees of order, the packing density and the surface coverage of the SAM monolayer all decrease as the alkyl chain length decreases.

Mixed SAMs are also widely used to fabricate biosensors by coadsorption of different surface-active organic species. Both the chemical composition and phase behavior of mixed SAMs have been widely reported in the literature. For example, a series of mixed-component SAMs with different chain length or different functionality were studied by Whitesides and coworkers[53-57], who found that the surface composition of the resulting "mixed" monolayers was different but proportional to the mole ratio of the mixture in the solution from which the SAM was assembled.

1.2.2 Characterization of monolayers

Many different thin film characterization techniques have been applied to determine the macroscopic characteristics of SAM monolayers. In spectroscopy-based techniques,

various technique utilizing different approaches and energy scales have been used to reveal information on their structure and growth. For example, Fourier transform infrared spectroscopy (FT-IR) uses the transition dipoles associated with vibrational modes to examine the orientation, order, and gauche defects[6,58,59], while X-ray photoelectron spectroscopy (XPS) evaluates the composition of the bound species[6] and diffraction-based techniques such as low-energy electron diffraction (LEED)[60], low-energy atom diffraction (LEAD)[61] and X-ray (and neutton) diffraction have been applied to examine the 2D structure of SAMs to investigate the physical structures of assemblies. In microscopy-based techniques, the scanning tunneling microscope (STM)[62], atomic force microscope (AFM)[63] and the lateral force microscope (LFM)[64,65] have all been used to study the organization of SAMs on substrates on the nanometer scale and can provide a direct image of the structure, revealing any defects or mixtures of different structures present during growth. STM usually offers a better spatial resolution than AFM, but reasonable tunneling currents for the STM through hydrocarbon chains are only possible for chain lengths of no more than 12 C atoms. Besides the techniques mentioned above, many others methods have been used, including ellipsometry measurement[66] and surface plasmon resonance (SPR)[67,68] to determine film thickness or coverage; contact angle goniometry to measure the surface energies and wetting behavior[47]; electrochemistry to probe electron transport through the SAM and to examine structural defects such as pinholes[69-72]; quartz crystal microgravimetry (QCM) to measure the kinetics of monolayer assembly[63] and temperature programmed desorption (TPD) to probe the thermodynamic aspects of adsorption and desorption and to determine bond strengths within the assembly.[73,74]

In overall characteristics, early molecular-level resolution diffraction studies of the structure of alkanethiolates monolayers on Au (111) surface[61,75,76] revealed that a hexagonal (√3×√3) R30° structure corresponds to a head-head (molecule-molecule) spacing of ~5Å and an area per molecule of 21.6Å^2. Atomic force microscopy (AFM)[77] and Helium diffraction[61] have been used to confirm the structure of alkanethiols on Au (111). Investigations of the "2D structure" (i.e., the structure projected onto the surface plane) describe the type (or absence) of crystalline long-range order, the symmetry, the lattice parameters, the packing in the plane, and the structure of the molecular backbone, including the possible tilt angle with respect to the surface normal, the tilt direction and the twist angle, are shown in Scheme.1.1.[78] In a projection onto a 2D plane, a straight hydrocarbon chain covers an area of 18.4 Å^2.[79] Assuming the full-coverage phase corresponds to the highest possible packing density, this suggests that the title angle θ_t between the axis of the hydrocarbon chains and the surface normal is around 32°, which is consistent with the early IR studies, an angle of trans segment rotation (twist) of the C-C-C planes about the molecular axis ψ of ~ 55°, and a tilt direction of the hydrocarbon chains χ_t derived from projection of molecule in substrate plane of ~13.8°.[80] Recently, by ultrahigh vacuum STM,[81-83] LEAD [84]and GIXD [85]studies, the existence of a C (4×2) superlattice with a (√3×√3) R30° structure was observed. The rectangular unit cell, with dimensions of 9.994 Å × 8.655Å, is about four times larger than that of the (√3×√3) R30° structure.

Although the surfaces are mostly full-coverage, where the monolayer completely covers the metal surface, very low concentrations of the pinholes normally present on a surface is revealed by STM[86-88] and AFM[89] studies. The pinholes in a monolayer

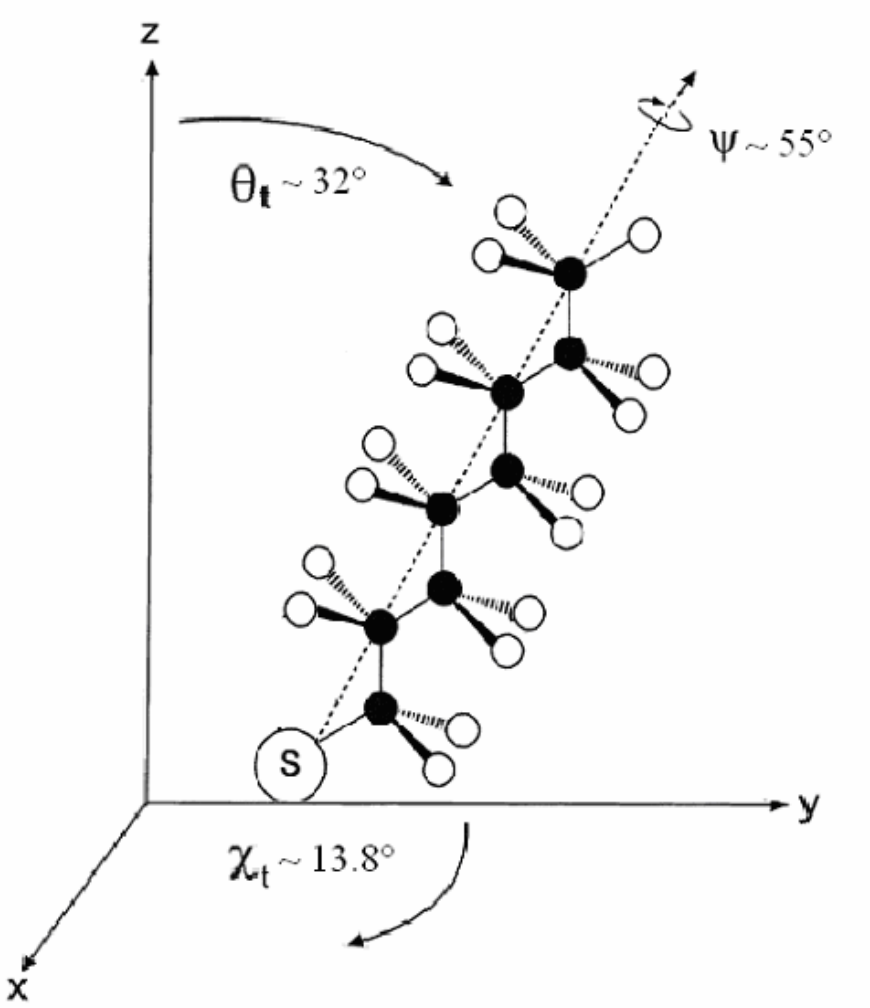

Scheme 1.1. Schematic of an alkanethiol molecule in all-trans conformation. Angle θ_t refers to the tilt of the molecular axis with respect to the substrate surface normal. χ_t defines the tilt direction, i.e., it is derived from projection of the molecule in the substrate plane. χ_t is undefined for $\theta_t = 0$. Twist angle, ψ, describes the rotation about the axis of the molecule.

covering the gold surface can be easily detected by electrochemistry.[70] Due to surface oxidation, a bare gold electrode in an acidic aqueous solution generates a well defined set of current peaks. After the gold electrode has been modified with SAM, the Faradaic current of a redox couple will decrease markedly, and may even disappear. A small residual current (residual oxidation) is caused by pinholes in the SAM or defect structures in the gold surface and provides a strong indication of the presence of pinholes.

1.3 Designing SAMs for biosensors

Functionalization and patterning of alkanethiol SAMs is one of the best methods currently available to immobilize macromolecular units such as proteins or enzymes onto a solid surface for fabricating biosensors, due to the simple preparation of the SAM film, and its reproducibility, stability and flexibility particularly its versatility due to the wide range of surfaces that can be created by incorporating different groups at the end of the alkyl chains at the monolayer interface.

1.3.1 Formation of self-assembled protein monolayers

Two basic immobilization approaches are generally utilized to couple the biomolecule to the SAM surface. The first approach is noncovalent coupling between the monolayers and the biomolecules via electrostatic, hydrophobic and hydrophilic interactions. In the second method, the biomolecule is chemically immobilized onto the SAM via the covalent attachment of the biomolecule to the surface of a monolayer containing free terminal groups such as amines through amide linkage formations or a cross-linking with the surface functional groups. Two different procedures are available

for the chemical immobilization of the bimolecules.[90] One is biomolecular modification, where the biomolecule of interest is tagged in solution with an appropriate sulfur-containing molecule through the specific reactive groups present on the biomolecule surface. The modified biomolecule is then self-assembled onto a solid substrate via the sulfur moiety. The other option is substrate modification, which is most extensively used. Here, the substrate is modified by coating it with self-assembling sulfur-based molecule. Subsequently the protein is combined with the SAM monolayer due to specific binding between the biomolecule surface and the SAM surface.

1.3.2 Advantages and limitations of SAMs for biosensors

A number of advantages for biosensor performance are offered by using SAM as a platform for linking biomolecules, either using direct chemical linkages or by encapsulation with the help of polymer supports. These are: (1) the simplicity of formation of ordered, stable and pinhole free monolayers; (2) versatile, low cost and stable alternatives to surface modification using organic monolayers with various functional groups; (3) only minimum amounts of the biomolecule (monolayer) need be immobilized on the SAM monolayer; (4) the SAM surface is suitable for orientational immobilization of biomolecules without altering their biological activities; (5) the ease of regeneration of the biosensors; (6) the reproducibility of the assay, as well as the inhibition of nonspecific adsorption; and (7) the ability to provide molecular level information about phenomena such as protein adsorption, antibody/antigen interaction, or DNA hybridization. using surface sensitive techniques such as STM and AFM. However, although SAM technology offers a useful and powerful tool for the sensor performance,

there still are several limitations of SAM for biosensors. First, immobilized enzymes are very sensitive to changes in the ionic strength, solution pH and temperature. The biological activity of the enzymes can sometimes be lost by a minor change in one of these parameters. Secondly, the chemical stability of some SAMs is not adequate, as the monolayer maybe chemically oxidized. Thirdly, due to high surface energy, contaminants can be adsorbed onto the hydrophobic SAM surface. These unwanted impurities may block the analyte recognition sites and thus lead to a decrease in the surface activity. Finally, the electric field induced and the thermal desorption of the monolayers is detrimental to biosensor applications.

1.4 Applications

Self-assembled monolayer technology sensors using SAMs have been applied for detection of pH,[91] inorganic molecules[92,93] and organic species[94-97] using both chemical and biological recognition elements. Especially, the most frequent application of SAM modified electrodes has been to monitor biomolecules and many SAM based biosensors have been studied. Based on the mechanism used for analyte recognition, SAM based biosensors can be generally classified into several types, namely electrochemical, optical, thermal and mass sensors, which are identified by the type of signal they generate.

1.4.1 Electrochemical sensors

According to the primary electric signal used to detect the analyte concentration, SAM based electrochemical sensors can be classified into: (a) potentiometric (voltammetric); (b) amperometric; and (c) conductimetric (impedometric), which are

relative to current measurement with time and afford very useful kinetic information for variety of redox active enzymes and proteins. SAMs based on thiols or related compounds are stable and are not desorbed from electrode surfaces within the potential range from -1400 to +800 mV vs. SCE in dilute sulfuric acid solutions. Consequently, SAMs can either be used to investigate a non-electroacive surface, or a selective electroacitive surface. At a non-electroactive surface, capacitance measurement is used to study the blocking properties of a SAM. A pinhole-free monolayer is impermeable to aqueous ions, and can act as an ideal capacitor.[76] Compared to a bare gold electrode, a SAM-covered electrode causes a strong decrease in electrode/electrolyte capacitance and decreases the electron-transfer rates used for kinetic studies.[98] Differential capacitance measurements are less sensitive than voltammetry, but make it possible to determine the film thickness and the permeability for simple ions. An electroactive SAM surface consists of blocking behavior and selective electron-tunneling or a 'gate', for the analyte as a suitable substrate for monitoring biomolecular interactions. After the thiol monolayers have been modified with redox active species, which will give SAM an electroactive background, the redox active end group (mediator for electron tansfer) of SAM can transfer the electrons between the redox center of the biomolecules and the electrode surface, which is pointed to an appropriate working electrode. Several mediators, such as ferrocene derivatives,[99,100] dimethylviologen,[101] N,N'-bipyridinium derivatives,[102] can be sued to facilitate the signal transmission of electrochemical sensors.

Amperometric biosensors, which can detect glucose, amino acids, glutathione and DNA from biological samples, are a significant application of SAM–based electrochemical biosensors. The first generation of amperometric biosensors utilizes

freely-diffusing natural redox mediators such as molecular oxygen or NAD^+ as mediated electron transfer shuttles between the enzyme and the transducer of biosensors.[103,104] In the second generation of amperometric biosensors artificial redox mediators such as ferrocene derivatives and quinines have been used for reduction and oxidation at the metal surface instead of the natural mediators.[105,106] In the third generation of amperometric sensors direct communication between the enzyme and electrode is provided by immobilizing the enzyme molecule in the SAM monolayer on an electrode surface.[107,108] SAMs based on amperometric sensors make the electron transfer distance between an immobilized redox enzyme and a suitable electrode surface as short as possible, and optimize the design of suitable surfaces for an anisotropic and oriented immobilization of enzymes on the SAM monolayer to increase the rate of electron transfer and the sensor signal.

Use of a carboxylic acid-terminated SAM surface [$HS(CH_2)_nCOOH$ with n of between 11 and 15] adsorbed with cytochrome-*c* (a mediator in cell redox reactions) using a carbodiimide reaction has provided an important development for SAM based amperometric biosensors.[109] Compared to electrostatically adsorbed cytochrome-*c*, carbodiimide-mediated attached molecules cannot be desorbed by a saturated potassium nitrate solution. Also, by using carboxylic acid-terminated SAMs (n=2, 5, or 10), dopamine sensors to detect the neurotransmitter dopamine in the presence of ascorbic acid have been developed, based on the condition that at neutral pH, negatively charged SAMs repel ascorbic acid while the positively charged dopamine can be measured at sub-millimolar level without any interference.[110] Several redox enzymes such as glucose oxidase linked SAMs, either with or without redox mediators have been used to fabricate

biosensors. A glucose sensor is prepared by crosslinking between the glucose oxidase (GOx) with a SAM from ω-hydroxy alkanethiol by glutaric diadehyde, and a redox mediator such as a ferrocene derivative provides the electrical communication between the electrode and GOx.[111] The sensitivity of the resulting enzyme electrode is related to the number of enzyme layers assembled onto the electrode. So, the sensitivities of these monolayer electrodes and the resulting amperometric signals are likely to be low due to the limited amounts of enzyme that can be attached as a monolayer to the electrode surfaces. To enhance these sensitivities, Riklin and Willner[112] successfully introduced the stepwise construction of a multilayer network of redox enzymes on a base SAM of thiolate attached to Au electrodes to develop a glucose biosensor and a bilirubin amperometric biosensor. Recently, SAM based electrochemical biosensors have been applied for the detection of specific DNA sequences,[113] the amount of DNA adsorbed onto an electrode surface,[114] and the binding of single strand[115] and double strand DNA to a monolayer of single strand oligonucleotoids.[116] There are two main reasons why self-assembled monolayers are attractive for DNA detection. First, end-point immobilization of DNA, which can be performed easily by synthesizing DNA with an alkanethiol linker at either the 5' or 3' end of DNA, is desirable to allow hybridization to occur efficiently. Secondly, a mixed monolayer of thiolated DNA and an alcohol terminated SAM[117] can orientate the immobilized single strand DNA away from the electrode surface, leading to an increased at hybridization efficiency.

1.4.2 Surface plasmon resonance sensors

Several optical SAM based biosensors, such as optical diffraction sensors, optical biosensors based on FTIRS, Self-Assembled Fluorescent sensors and surface plasmon resonance sensors, have been applied and discussed in the literature. RAIRS based sensors are ideally suited for the study of protein SAMs deposited on metal surface, because this surface specific infrared technique can not only detect the presence of self-assembled proteins on the metal-coated substrate, but can also be used to determine the outcome of reactions occurring at SAM surfaces.[90] Since B. Leidberg, et al. first introduced surface plasmon resonance for biosensing sensors in 1983, biosensors based on surface plasmon resonance have found a very wide variety of applications and have contributed to thousands of scientific publications on biomolecular interactions due to their high accuracy and reliability. This optical technique monitors changes in the thickness of the monolayer coverage of a metal surface to study the biomolecular interaction between the biological sensing element, an immobilized biorecognition molecule, and the target analyte. Compared to the conventional techniques used for studying biomolecular interactions, such as immunoassays (ELISA or RIA), equilibrium dialysis, affinity chromatography and spectroscopy, SPR methods offers two main advantages: binding events are monitored in real-time and these are very sensitive, label-free biochemical assays.

When a *p*-polarized laser beam is totally internally reflected at the interface of two optical mediums with different refractive indexes, an evanescent field is generated. At a specific angle (the resonance angle) of incidence, the field is enhanced and an SPR signal is observed as a minimum in reflectance caused by the absorption of photons when the

energy supplied by the laser excites the surface plasmons into resonance (a collective motion of conducting electrons) in a thin (≈ 50 nm) metal layer. The resonance angle is highly dependent on changes in the refractive index at the metal/air or metal/solution interface. SAMs are ideally situated to interact with the strongest part of the evanescent wave of an SPR system. From the shifts in the reflectance minima and Fresnel's equations, the thickness of the SAM on the metal surface can be calculated.[118,119] Gold and silver surfaces are commonly used due to their low imaginary dielectric constant. When large target biomolecules are deposited on SAM surfaces coated with binding biomolecules, which may be antibodies, DNA probes, enzyme or other reagents chosen because they react exclusively with the selected target molecule, the concentrations of specific target molecules can be quantitatively measured by observing the resulting of large shifts in the value of the SPR minimum. In a typical instrument for SPR biosensing, a glass slide with a thin gold coating is mounted on a prism. A laser light beam passes through the prism and slide, reflects off the gold and passes back through the prism to a detector. Changes in reflectivity *vs* angle or wavelength give a signal that is proportional to the volume of biopolymer bound near the surface. A flow cell allows solutions above the gold surface to be rapidly changed.

A versatile and useful biotin-functionalized SAM based SPR biosensor has been reported by Knoll and coworkers.[120,121] Biotin (vitamin H) has an extremely high binding constant and the biotin modified monolayers bind streptavadin very effectively, which can then be attached with a biotinylated antibody (anti-hCG). The mixture of biotinylated long-chain alkanethiols and shorter hydroxythiols used to dilute the monolayer thus

optimizes the effectiveness of binding to streptavitin. The long-chain alkanethiol acts as spacer molecule, elevating the biotin group above the monolayer surface.

The SPR technique is highly useful for monitoring the in situ growth of SAMs as well as its host-guest interactions in solutions with appropriate molecules. Long-chain SAM surfaces modified with cyclodextrins, which are cyclic oligosaccharides, or with calix[4]arenes are highly selective ways to chelate small organic molecules as well as larger biologically relevant guest molecule in their cavity. Derivatised with multiple long-chain thiol spacers, the cyclodextrin molecules are assembled parallel to the surface. In this orientation they are freely accessible for dye molecules.[122] Reinhoudt and coworkers[123-125] have reported that calixe [4]arene modified SAM surfaces are also capable of binding large steroids such as corticoaterne-21-acetate, cortisone-21-acetate and prednisolene-21-acetate.

By creating micelles that act as artificial lipid layers or lipid membranes with entrapped gangliosides, specific recognition with a high sensitivity for cholera toxin has been achieved with a detection limit of up to 10^{-9} M with SPR. Micelles of lipid (membrane) can be easily immobilized on a SAM of an alkanethiol through hydrophobic interaction.[126] Detection of similar biomolecular interactions such as DNA hybridization[127] and antigen-antibody[128] have been achieved by SAM based SPR sensors.

1.4. 3 Quartz crystal microbalance

A quartz crystal microbalance biosensor is an ultra-sensitive mass sensor with the ability to measure a wide range of mass change on a quartz crystal resonator in real time. At the low mass end, is can detect monolayer surface coverage by small molecules or

polymer films. At the upper end, it is able to detect much larger masses bound to the surface. These can be complex arrays of biopolymers and biomacromolecules, even whole cells.

The heart of the QCM is the piezoelectric quartz crystal wafer, with different thicknesses sandwiched between a pair of electrodes that provide a means of connecting the device to an external oscillator circuit that drives the quartz crystal at its resonant frequency due to the piezoelectric effect. The quartz crystals are mass-sensitive transducers; their frequency is dependent on the mass of the crystal's surface as well as the mass of any layers confined to the electrode areas of the crystal. Changes in the crystal frequency reflect tiny changes in the mass on the electrode's surface. In 1959, Sauerbray[129] discovered the linear relationship between the frequency responses of an oscillating piezoelectric crystal and the mass deposited on the crystal. The frequency-to-mass relationship is described by the Sauerbray equation:

$$\Delta f = -C_f \Delta m$$

Where Δf is the change in the oscillation frequency of the coated crystal, f is the fundamental frequency of the crystal, C_f is the sensitivity factor, and Δm is the change in the mass adsorbed onto the crystal surface.

Early QCM was chemically applied to measure mass binding from gas-phase species to the crystal surface.[130] In the 1980s, solution based QCM was developed as new oscillator technology made it possible to detect changes in the frequency related to changes in viscosity and density in highly damping liquid media.[131,132] QCM biosensors based on self-assembled monolayers represent a relatively new class of devices to which biological recognition elements have been attached. SAM is used as an interface layer

between a piezoelectric quartz crystal surface and solution or vapor to improve the specificity of QCM biosensors. The benefits of QCM biosensors based on SAMs have allowed a number of biological systems like enzyme immobilization and selective sensing for small organic or large biomolecules to be studied. For example, for the determination of human chorionic gonadotropin,[133] the anti-hCG antibody is immobilized on the surface of gold electrode of 10 MHz quartz AT-cut crystal by self-assembling techniques using sulfosuccinimidy 6-[3'-(2-pyridyldithio)propionamido] hexanoate, and serves as an antibody recognizing layer. The highly ordered thiolate SAM on the crystal surface leads to orientational immobilization of the antibody/antigen without altering the biological activities. Compared with conventional antibody immobilization methods, this technique offers many advantages for sensor performance, including improving the binding activity of the antibody monolayer, wider detection limits, easy regeneration of the biosensors, a reproducible assay, and the inhibition of nonspecific adsorption. For example in the detection of DNA hybridization, Satjapipat and coworkers[134] used a gold QCM surface modified with a mixed monolayer of reduceable thiol (mercaptopropionic acid) and oligonucleotide derivatized mercaptoprohexylthiol, where the mercaptoprohexythiol was used for the oligonucleotide attachment and subsequent DNA hybridization. After the monolayer was assembled, they reduced the mercaptopropionic acid, which caused it to be desorbed. Compared to self-assembling the pure oligonucleotide derivatized mercaptoprohexylthiol monolayer, this method increased the efficiency of DNA hybridization in the subsequent step by an order of magnitude due to the bare gold's effect on reducing DNA surface density and promoting a better oligonucleotide orientation for hybridization.

To develop a label-free, time-efficient, quantitative immunoassay, surface plasmon resonance spectroscopy and the quartz crystal microbalance are of particular interest to researchers. Both techniques utilize wave propagation phenomena: SPR uses optical waves and detects the angle of the reflection minimum, while QCM makes use of acoustic waves and measures the frequency of the acoustic impedance minimum. Similar advantages for both techniques are obtained in terms of detection limit, sensitivity, flow capabilities, and speed of real–time detection. However, compared to the complicated and expensive optics needed by commercial SPR, QCM is low cost and easy to use. Another advantage is its ability to work with 3D substrates and multilayer adsorptions.

1.5 Inhibition of nonspecific adsorption on biosensors

The biological recognition system in biosensors can capture picomolar concentrations of specific analytes from biological samples through specific binding interactions (specific adsorption). However, many biomolecules such as proteins or cells have a tendency to adsorb onto interfaces between solid substrates and biological sample solutions without specific receptor-recognition interaction (nonspecific adsorption). The reasons why biomolecules adsorb nonspecifically at solid and water interfaces are: (1) the underlying solid substrate of an immunosensor is highly hydrophobic, highly ionic, or has highly hydrogen bonding; (2) hydrophobic surfaces in water form high energy interfaces; (3) most biomolecules have hydrophobic patches on their surface, such as protein itself which has loops, tails helices and sheets that can be oriented toward the substrate; and (4) there is a thermodynamic driving force that minimizes high solid and water interfacial energy by adsorbing surface-active molecules such as proteins. Such adsorption often

brings together hydrophobic regions on protein and hydrophobic surface regions, with the consequent release of water molecules.

An essential characteristic of an immunosensor is that its surfaces must block the adsorption of microorganisms, other thatn the target organism. The sensitivity of many transducers of biosensors, such as surface plasmon resonance, electrochemical impedance spectroscopy, contact angle measurements and surface vibrational spectroscopy is thus determined by the nonspecific adsorption of immunoactive organisms. These detections detect the presence of organisms, but cannot distinguish between the target organism and nontarget organisms that are adsorbed on the surface. Nonspecific adsorption typically reduces the functionality of a biosensor interface, which is used in biorecognition, by producing undesirable features like high background noise or false positive results in diagnostic tests. Consequently, an important challenge for biochemists is to create nonfouling surfaces for many biotechnology applications. These surfaces require both enhanced specific adsorption and reduced nonspecific adsorption to give biosensors a biomolecule–resistant background. Due to the hydrophobic and charged characters of most biomolecules, they do not adsorb strongly at neutral hydrophilic interfaces and at interfaces of the same charge. Based on these observations and principles of nonspecific adsorption, a wide range of hydrophilic synthetic and natural polymers or coating compositions have been designed for use as non-fouling surfaces. In natural hydrophilic surfaces that resist protein and cell adhesion, several compositions of nonfouling surface have been used, such as passivating protein monolayers (albumin, casein), glycoproteins (mucins), polysaccharides (dextran, hyaluron acid).[135] Due to the naturally low affinity of these natural biomolecules with components of body fluids and tissues, a widely

employed approach of inhibition of protein adsorption is to use a blocking solution containing a protein such as bovine serum albumin (BSA).[136] However, problems such as the denaturation of the blocking protein over time or exchange of this protein with others in solution are experienced in this approach. A polymer coating or self-assembled monolayer surface with biomolecular nonspecific adsorption resistant characteristics is used for many biological applications. In these synthetic hydrophilic surfaces, the compositions may be PEG polymers; neutral polymers (PHEMA, PAAm); gas discharged deposited coatings (tetraglyme); oligoEGs; zwitterions; or other groups on SAMs.[135]

1.5.1 Poly(ethylene glycol) (PEG)

Due to its ability to inhibit protein and cell adhesion, as well as its nontoxic and nonimmunogenic character, poly(ethylene glycol) (PEG) has been extensively used for many biological applications.[137] In the late 1960s, the idea of PEGlating surfaces was proposed by Frank Davis and in the late 1970s Ed Merrill at MIT began to study PEG hydrogels. By the early 1980s, surface-grafted PEG-based materials have begun to be used to prevent protein adsorption from biological media.[138] PEG coating surfaces can be made by several methods, such as the formation of PEG hydrogels using a polymerizable PEG resin; chemical immobilization through direct attachments to surfaces; graft polymerization of PEG monomers to a polymer backbone; and adsorption of PEG block copolymers at multiple sites on the surfaces. Nonfouling behavior of the PEG coating surface is generally ascribed to the steric repulsion effect, where the polymer prevents the protein from reaching the surface to be adsorbed. The balance between steric repulsion, van der Waals attraction, and the hydrophobic interaction between proteins in the

biological sample and the PEG surface haws also been addressed by Jeon et al.[139,140] In the late 1980s, Graham found that two water molecules are H-bonded to each PEG ether group, which is a well-known proton acceptor. This discovery was used to explain the capacity of PEG surface to resist protein and cell adhesion. The steric repulsion has both osmotic and elastic components; the elastic component is caused by the compression and restriction of the ethylene oxide chains/segments, while the osmotic component is caused by the loss of "water of hydration". These components come into play, as the protein reaches the substrate by diffusion and compresses the PEG layer. As the van der Walls contribution to the attractive force is smaller than the hydrophobic interaction between the protein and the hydrophobic surface, only the hydrophobic interaction is thought to compete with the steric repulsion. The steric repulsion effect of the inhibition of protein adsorption on the surface is related to the positive free energy associated with compression and concomitant desolvation. The mechanisms of nonfouling PEG on surfaces are shown in Scheme 1.2. When a protein molecule attempts to be adsorbed onto the surface, the coil of PEG chains is compressed and water associated with PEG chain is released into the bulk solution. This will lead to an increase in enthalpy due to chain dehydration and a decrease in entropy due to chain compression**.** Both changes lead to an increase in the free energy of total system, which is thermodynamically unfavorable. The osmotic pressure created by the steric repulsion inside the coil, the driving force for diluting the polymer concentration draws water back into the coil to minimize the free energy of the total system and thus repels the protein molecule.

Many physical parameters such as PEG's large excluded volume in aqueous solution, configurational entropy, hydrated chain mobility, molecular weight,[141] the

surface density of PEG,[142] and the protein size and charge could affect the effectiveness of PEG coating surfaces providing resistance to nonspecific adsorption. Fibrinogen adsorption as a function of PEG molecular weight with 400, 1000, 3500 and 20,000 MW has been discussed by Hoffman and Gombotz.[141] As the molecular weight of PEG increased, the amount of fibrinogen adsorbed on the surface decrease quite rapidly at first, up to a PEG molecular weight of 3500. A further increase in PEG MW up to 20,000 resulted in only a slight decrease in fibrinogen adsorption. They concluded that at a PEG molecular weight of between 2000 and 3500 is the optimal range for inhibition of fibrinogen adsorption. Unsworth et al.[142] reported that a reduction in the fibrinogen adsorption on gold surfaces modified with 750MW and 5000MW PEO was affected by

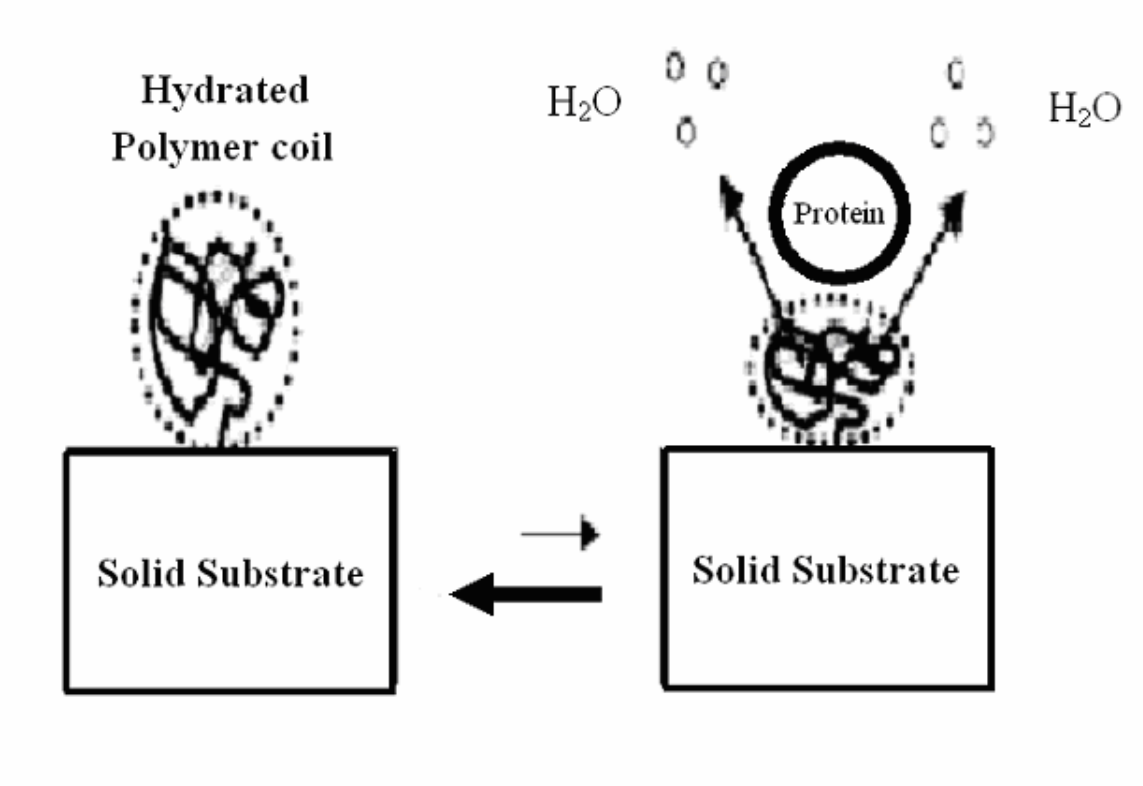

Scheme 1.2. Schematic illustration of the mechanisms of nonfouling PEG on surfaces

the chain density of PEG measured by ellipsometry, and concluded that by chain density plays a major role in the resistivities of PEG-coated surfaces and that PEG molecules with different molecular weights may have different optimum surface densities for reducing nonspecific adsorption. Hoffman[135] also studied the effect of protein size for protein adsorption on surfaces modified with PEG and showed that when the molecular weight of the protein was less than 10K Dalton, protein adsorption occurred on PEG-coated surfaces. Because there are gaps between PEG chains, proteins with small molecular weights can penetrate the layer of PEG chains and be adsorbed onto the surface. The fabrication of PEG coating surfaces with optimal selectivity, biocompatibility and minimal nonspecific binding is therefore critical for the development of many diagnostic and biosensing applications.

1.5.2 Oligo(ethylene glycol) (OEG)-terminated SAMs

In the early 1990s, the use of oligo(ethylene glycol) (OEG) terminated alkanethiolate self-assembled monolayers [$HS(CH_2)_{11}(OCH_2CH_2)_nOH$: n=2-17] was first described for inhibiting protein adsorption by Prime and Whitesides.[143-145] In these more densely packed, shorter oligo(ethylene glycol) (OEG)-terminated SAMs, the OEG-SAMs have less conformational freedom to lose, upon protein adsorption than the less densely packed, longer PEG chains. Consequently their capacity to resist protein and cell adsorption is generally attributed to the osmotic component of the steric repulsion model. The water barrier theory is generally used to explain the non-fouling behavior of the OEG-SAM surface; that is, the protein cannot be adsorbed onto the OEG surface because there is a layer of tightly bound water molecules around the OEG chains.[146-150] Therefore, the

resistance of OEG-SAMs to the adsorption of protein is mainly due to the difficulty in dehydrating both ethylene glycol chains and the protein and is related to the amount of hydrogen bonds (or the mobility of OEG chains); so, the highly mobile and highly hydrated OEG-SAMs have better nonfouling properties. Recently, Vandereah et al.[151-153] and Li et al.[154] found that methoxy-terminated OEG-SAM surfaces with higher surface packing density or more ordered structures have higher protein adsorption, and used with different assembly solvents, such as 95% ethanol and water, can form either ordered or disordered methyl-terminated OEG-SAMs. They also reported that the extent of OEG-SAMs' resistance to nonspecific adsorption depends not only on the packing density but also on the number of the repeat EG unit.

1.6 References

1. Byfield, M. P.; Abuknesha, R. A. *Biosens. Bioelectron.* **1994**, *9*, 373.

2. Khilko, S. N.; Corr, M.; Boyd, L. F.; Lees, A.; Inman, J. K.; Margulies, D. H. *J. Bioll Chem.* **1993**, *268*, 15425.

3. Sadana, A.; Beelaram, A. M. *Biosens. Bioelectron.* **1995**, *10*, 301.

4. Schubert, D. W. *Polym. Bull.* **1997**, *38*, 177.

5. Kaganer, V. M.; Mohwald, H.; Dutta, P. *Rev. Mod. Phys.* **1999**, *71*, 779.

6. Ulman, A. *An Introduction to Ultrathin Organic Films: From Langmuir-Blodgett to Self-Assembly, Academic Press, Boston,* **1991**.

7. Forrest, S. R. *Chem. Rev.* **1997**, *97*, 1793.

8. Umbach, E.; Sokolowski, M.; Fink, R. *Appl. Phys. A* **1996**, *63*, 565.

9. Fenter, P.; Schreiber, F.; L. Zhou; Eisenberger, P.; Forrest, S. R. *Phys. Rev. B* **1997**, *56*, 3046.

10. Allara, D. L.; Nuzzo, R. G. *Langmuir* **1985**, *1*, 45.

11. Allara, D. L.; Nuzzo, R. G. *Langmuir* **1985**, *1*, 52.

12. Ogawa, H. C., T.; Taya, K. J. *J. Am. Chem. Soc.* **1985**, *107*, 1365.

13. Sagiv, J. *J. Am. Chem. Soc.* **1980**, *102*, 92.

14. Silberzan, P. L., L.; Ausserré, D.; Benattar, J. J. *Langmuir* **1991**, *7*, 1647.

15. Wasserman, S. R.; Tao, Y.-T.; Whitesides, J. M. *Langmuir* **1989**, *5*, 1074.

16. Le Grange, J. D.; Markham, J. L.; Kurjian, C. R. *Langmuir* **1993**, *9*, 1749.

17. Maoz, R.; Sagiv, J. *J. Colloid Interf. Sci.* **1984**, *100*, 465.

18. Gun, J.; Sagiv, J. *J. Colloid Interf. Sci.* **1986**, *112*, 457.

19. Carson, G.; Granick, S. *J. Appl. Polym. Sci.* **1989**, *37*, 2767.

20. Kessel, C. R.; Granick, S. *Langmuir* **1991**, *7*, 532.

21. Schwartz, D. K.; Steinberg, S.; Israelachvili, J.; Zasadzinski, Z. A. N. *Phys. Rev. Lett.* **1992**, *69*, 3354.

22. Gun, J.; Iscovici, R.; Sagiv, J. *J. Colloid Interf. Sci.* **1984**, *101*, 201.

23. Tillman, N.; Ulman, A.; Schildkraut, J. S.; Penner, T. L. *J. Am. Chem. Soc.* **1988**, *110*, 6136.

24. Dubois, L. H. N., R. G. *Ann. Phys. Chem.* **1992**, *43*, 437.

25. Bain, C. D.; Whitesides, G. M. *Adv. Mater.* **1989**, *1*, 506.

26. Lee, T. R.; Laibinis, P. E.; Folkers, J. P.; Whitesides, G. M. *Pure Appl. Chem.* **1991**, *63*, 821.

27. Whitesides, G. M.; Ferguson, G. S. *Chemtracts-Org. Chem.* **1988**, *1*, 171.

28. Troughton, E. B.; Bain, C. D.; Whitesides, G. M.; Allara, D. L.; Porter, M. D. *Langmuir* **1984**, *4*, 365.

29. Katz, E.; Itzhak, N.; Willner, I. *J. Electroanal. Chem.* **1992**, *336*, 357.

30. Nuzzo, R. G.; Allara, D. L. *J. Am. Chem. Soc.* **1983**, *105*, 4481.

31. Sabatani, E. C.-B., J.; Bruening, M.; Rubinstein, I. *Langmuir* **1993**, *9*, 2974.

32. Bryant, M. A.; Joa, S. L.; Pemberton, J. E. *Langmuir* **1992**, *9*, 753.

33. Hill, W.; Wehling, B. *J. Phys. Chem.* **1993**, *97*, 9451.

34. Li, T. T.-T.; Liu, H. Y.; Weaver, M. J. *J. Am. Chem. Soc.* **1984**, *106*, 1233.

35. Cooper, J. M.; Greenough, K. R.; McNeil, C. J. *J. Electroanal. Chem.* **1993**, *347*, 267.

36. Uvdal, K.; Bodo¨, P.; Liedberg, B. *J. Colloid Interf. Sci.* **1992**, *149*, 1233.

37. Ihs, A.; Uvdal, K.; Liedberg, B. *Langmuir* **1993**, *9*, 733.

38. Arndt, T.; Schupp, H.; Schepp, W. *Thin Solid Films* **1989**, *178*, 319.

39. Mielczarski, J. A.; Yoon, R. H. *Langmuir* **1991**, *7*, 101.

40. Edwards, T. R. G.; Cunnane, V. J.; Parsons, R.; Gani, D. *J. Chem. Soc., Chem. Commun.* **1989**, 1041.

41. Arduengo, A. J.; Moran, J. R.; Rodriguez-Paradu, J.; Ward, M. D. *J. Am. Chem. Soc.* **1990**, *112*, 6153.

42. Xue, G.; Huang, X.-Y.; Dong, J. Z., J. *J. Electroanal. Chem.* **1991**, *310*, 139.

43. Bharathi, S.; Yegnaraman, V.; Rao, G. P. *Langmuir* **1993**, *9*, 1614.

44. Samanat, M. G.; Broen, C. A.; Gordon, J. G. *Langmuir* **1992**, *8*, 1615.

45. Biebuyck, H. A.; Bain, C. D.; Whitesides, G. M. *Langmuir* **1994**, *10*, 1825.

46. Ulman, A. *Chem. Rev.* **1996**, *96*, 1533.

47. Bain, C. D.; Troughton, E. B.; Tao, Y. T.; Evall, J.; Whitesides, G. M.; Nuzzo, R. G. *J. Am. Chem. Soc.* **1989**, *111*, 321.

48. Nuzzo, R. G.; Allara, D. L. *J. Am. Chem. Soc.* **1983**, *105*, 4481.

49. Nuzzo, R.G.; Dubois, L. H. *J. Am. Chem. Soc.* **1987**, *109*, 733.

50. Sagiv, J. *J. Am. Chem. Soc.* **1980**, *102*, 92.

51. Li, L.Y.; Chen, S. F.; Zheng, J.; Ratner, B. D.; Jiang, S. Y. *J. Phys. Chem. B* 2005, *109*, 2934.

52. Losic, D.; Shapter, J. G.; Gooding, J. J. *Langmuir* 2001, *17*, 3307.

53. Bain, C. D.; Whitesides, G. M. *J. Am. Chem. Soc.* **1988**, *110*, 6560.

54. Bain, C. D.; Evall, J.; Whitesides, G. M. *J. Am. Chem. Soc.* **1989**, *111*, 7155.

55. Bain, C. D.; Whitesides, G. M. *J. Am. Chem. Soc.* **1988**, *110*, 3665.

56. Bain, C. D.; Whitesides, G. M. *J. Am. Chem. Soc.* **1989**, *111*, 7164.

57. Folkers, J. P.; Laibinis, P. E.; Whitesides, G. M. *Langmuir* **1992**, *8*, 1330.

58. Nuzzo, R. G.; Dubois, L. H.; Allara, D. L. *J. Am. Chem. Soc.* **1990**, *112*, 558.

59. Parikh, A. N.; Allara, D. L. *J. Am. Chem. Soc.* **1992**, *96*, 927.

60. Dubois, L. H.; Zegarski, B. R.; Nuzzo, R. G. . *Chem. Phys.* **1993**, *98*, 678.

61. Chidsey, C. E. D.; Liu, G. Y.; Rowntree, P.; Scoles, G. *J. Chem. Phys.* **1989**, *91*, 4421.

62. Poirier, G. E. *Chem. Rev. (Washington, D. C.)* **1997**, *97*, 1117.

63. Ulman, A. *Self-assembled monolayers of thiols, Thin Films, vol 24, Academic Press, San Diego* **1998**.

64. Piner, R. D.; Xu, F.; Hong, S. H.; Mirkin, C. A.*Science* **1999**, *283*, 661.

65. Wilbur, J. L.; Macdonald, J. C.; Whitesides, G. M. *Langmuir* **1995**, *11*, 825.

66. Wasserman, S. R.; Whitesides, G. M.; Tidswell, I. M.; Ocko, B. M.; Pershan, P. S.; Axe, J. D. *J. Am. Chem. Soc.* **1989**, *111*, 5852.

67. Aust, E. F.; Sawodny, M.; Ito, S.; Knoll, W. *Scanning* **1994**, *16*, 353.

68. Peterlinz, K. A.; Georgiadis, R. *Langmuir* 1996, *12*, 4731.

69. Porter, M. D.; Bright, T. B.; Allara, D. L.; Chidsey, C. E. D. *J. Am. Chem. Soc.* **1987**, *109*, 3559.

70. Finklea, H. O.; Avery, S.; Lynch, M.; Furtsch, T. *Langmuir* **1987**, *3*, 409.

71. Sabatani, E.; Rubinstein, I. *J. Phys. Chem.* **1987**, *91*, 6663.

72. Sabatani, E.; Rubinstein, I.; Maoz, R.; Sagiv, J. *J. Electroanal. Chem.* **1987**, *219*, 365.

73. Dubois, L. H.; Zegarski, B. R.; Nuzzo, R. G. *J. Am. Chem. Soc.* **1990**, *112*, 570.

74. Wetterer, S. M.; Lavrich, D. J.; Cummings, T.; Bernasek, S. L.; Scoles, G. *J. Phys. Chem. B* **1998**, *102*, 9266.

75. Strong, L.; Whitesides, G. M. *Langmuir* **1988**, *4*, 546.

76. Chidsey, C. E. D.; Loiacono, D. N. *Langmuir* **1990**, *6*, 682.

77. Alves, C. A.; Smith, E. L.; Porter, M. D. *J. Am. Chem. Soc.* **1992**, *114*, 1222.

78. Schreiber, F. *Progress in Surface Science* **2000**, *65*, 151.

79. Kitaigorodskii, A. I. *Organic Chemistry Crystallography, Consultants Bureau, New York, 1961.* **1961**.

80. Delamarche, E.; Michel, B.; Gerber, C.; Anselmetti, D.; Guentherodt, H. J.; Wolf, H.; Ringsdorf, H. *Langmuir* **1994**, *10*, 2869.

81. Poirier, G. E.; Tarlov, M. J. *Langmuir* **1994**, *10*, 2853.

82. Delamarche, E.; Michel, B.; Gerber, Ch.; Anselmetti, D.; Guentherodt, H.-J.; Wolf, H.; Ringsdorf, H. *Langmuir* 1994, *10*, 2869.

83. Bucher, J. P.; Santesson, L.; Kern, K. *Appl. Phys. A* **1994**, *59* 135.

84. Camillone, N., III; Chidsey, C. E. D.; Liu, G. Y.; Scoles, G. *J. Chem. Phys.***1993**, *98*, 4234.

85. Fenter, P.; Eisenberger, P.; Liang, K. S. *Phy. Rev. Lett.* **1993**, *70*, 2447.

86. Edinger, K.; Golzhaeuser, A.; Demota, K.; Woll, C., and Grunze, M., *Langmuir* **1993**, *9*, 4.

87. Sun, L.; and Crooks, R. M. *Langmuir* **1993**, *9*, 1951.

88. Delamarche, E.; Michel, B.; Kang, H.; Gerber, C. *Langmuir* **1994**, *10*, 4103.

89. Pan, J., Tao, N., and Lindsay, S. M., *Langmuir* **1993**, *9*, 1556.

90. Ferretti, S.; Paynter, S.; Russell, D. A.; Sapsford, K. E.; Richardson, D. J. *Trends Anal. Chem.* **2000**, *19*, 530.

91. Hickman, J. J.; Ofer, D.; Laibinis, P. E.; Whitesides, G. M.; Wrighton, M. S. *Science (Washington, DC, United States)* **1991**, *252*, 688.

92. Turyan, I.; Mandler, D. *Ana.l Chem.* **1994**, *66*, 58.

93. Turyan, I.; Mandler, D. *Ana.l Chem.***1997**, *69*, 894.

94. Gooding, J. J.; Hibbert, D. B. *Trends Anal. Chem* **1999**, *18*, 525.

95. Willner, I.; Katz, E. *Angew. Chem,- Int. Edit.* **2000**, *39*, 1181.

96. Gooding, J. J.; Erokhin, P.; Losic, D.; Yang, W.; Policarpio, V.; Liu, J.; Ho, F. M.; Situmorang, M.; Hibbert, D. B.; Shapter, J. G. *Anal. Sci.* **2001**, *17*, 3.

97. Gooding, J. J.; Erokhin, P.; Hibbert, D. B. *Biosens. Bioelectron.* **2000**, *15*, 229.

98. Finklea, H. O. *Electroananal. Chem.* **1996**, *19*, 109.

99. Gass, A. E. G.; Davis, G.; Hill, H. A. O.; Higgins, I. J.; Plotkin, E. V.; Turner, A. P. F.; Aston, W. J. *In: Allen, M.J., Usherwood, P.N.R. (Eds.), Charge and Field Effects in Biosystem. Abacus, Tunbridge Wells, UK,* **1984**, 475.

100. Davis, G.; Hill, H. A. O.; Higgins, I. J.; Turner, A. P. F. *In: Ko, W.H. (Ed.), Implantable Sensors for Clossed Loop Prosthetic Systems. Futura, New York,* **1985**, 189.

101. Hill, H. A. O.; Higgins, I. J. *Philosophical Transactions of the Royal Society of London, Series A: Mathematical, Physical and Engineering Sciences* **1981**, *302*, 267.

102. Willner, I.; Lapidot, N.; Riklin, A.; Kasher, R.; Zahavy, E.; Katz, E. *J. Am. Chem. Soc.***1994**, *116*, 1428.

103. Thevenot, D. R.; Sternberg, R. Coulet, P. *Diabetes Care* **1982**, *5*, 203.

104. Churchouse, S. J.; Battersby, C. M.; Mullen, W. H.; Vadgama, P. M. *Biosens.* **1986**, *2*, 325.

105. Kulys, J.; Cenas, N. K. *Biochem. Biophys. Acta* **1983**, *744*, 57.

106. Yokoyama, K.; Tamiya, E.; Karube, I. *J. Electroanal. Chem.* **1989**, *273*, 107.

107. A., A. F. *Adv, Inorg . Chem.* **1992**, *38*, 117.

108. Ghindilis, A. L.; Atanasov, P.; Wilkins, E. *Electroanalysis* **1997**, *9*, 661.

109. Collinson, M.; Bowden, E. F.; Tarlov, M. J. *Langmuir* **1992**, *8*, 1247.

110. Malem, F.; Mandler, D. *Analytical Chemistry* **1993**, *65*, 37.

111. Creager, S. E.; Olsen, K. G. *Analytica Chimica Acta* **1995**, *307*, 277.

112. Riklin, A.; Willner, I. *Analytical Chemistry* **1995**, *67*, 4118.

113. Ihara, T.; Nakayama, M.; Murata, M.; Nakano, K.; Maeda, M. *Chemical Communications (Cambridge)* **1997**, 1609.

114. pang, D. W.; Zhang, Z. L.; Qi, Y. P.; Cheng, J. K.; Liu, Z. Y. *J. Electroanal. Chem.* **1996**, *403*, 183.

115. Bardea, A.; Patolsky, F.; Dagan, A.; Willner, I. *Chem. Commun.* **1999**, 21.

116. Steel, A. B.; Herne, T. M.; Tarlov, M. J. *Anal. Chem.* **1998**, *70*, 4670.

117. Levicky, R.; Herne, T. M.; Tarlov, M. J.; Satija, S. K. *J. Am. Chem. Soc.* **1998**, *120*, 9787.

118. Gorddon II, J. G.; Swalen, J. D. *Opt. Commun.* **1977**, *22*, 374.

119. Aust, E.; Ito, S.; Sawodny, M.; Knoll, W. *TRIP* **1994**, *2*, 313.

120. Spinke, J.; Liley, M.; Guder, H. J.; Angermaier, L.; Knoll, W. *Langmuir* **1993**, *9*, 1821.

121. Spinke, J.; Liley, M.; Schmitt, F. J.; Guder, H. J.; Angermaier, L.; Knoll, W. *J. Chem. Phys.* **1993**, *99*, 7012.

122. Mitter-Neher, S.; Spinke, J.; Liley, M.; Nelles, G.; weisser, M.; Back, R.; Wenz, G.; Knoll, W. *Biosens. Bioelectron.* **1995**, *9*, 903.

123. Huisman, B. H.; Kooyman, R. P. H.; Van Veggel, F. C. J. M.; Reinhoudt, D. N. *Advanced Materials (Weinheim, Germany)* **1996**, *8*, 561.

124. Friggeri, A.; Van Veggel, F. C. J. M.; Reinhoudt, D. N.; Kooyman, R. P. H. *Langmuir* **1998**, *14*, 5457.

125. Friggeri, A.; Van Veggel, F. C. J. M.; Reinhoudt, D. N. *Chemistry--A European Journal* **1999**, *5*, 3595.

126. Terrettaz, S.; Stora, T.; Duschl, C.; Vogel, H. *Langmuir* **1993**, *9*, 1361.

127. Piscevic, D.; Lawall, R.; Veith, M.; Liley, M.; Okahata, Y.; Knoll, W. *Appl. Surf. Sci.* **1995**, *90*, 425.

128. Duschl, C.; Sevin-Landais, A.-F.; Vogel, H. *Biophys. J.* **1996**, *70*, 1985.

129. Sauerbray, G. *Z. Phys.* **1959**, *155*, 206.

130. Konash, P. L.; Bastiaans, G. J. *J. Anal. Chem* **1980**, *52*, 1929.

131. Nomura, T.; Okuhara, M. *Anal. Chim. Acta* **1982**, *142*, 281.

132. Kurosawa, K.; Tawara, E.; Kamo, N.; Kobatake, Y. *Anal. Chim. Acta* **1990**, *230*, 41.

133. Zhang, B.; Mao, Q. G.; Zhang, X.; Jiang, T. L.; Chen, M.; Fu, W. L. *Biosens. Bioelectron.* **2004**, *19*, 711.

134. Satjapipat, M.; Sanedrin, R.; Zhou, F. *Langmuir* **2001**, *17*, 7637.

135. Hoffman, A. S. *12th CIRMIB in biomedical Devices, Molecular recognition and Tissue Engineering* **2005**.

136. Huang, T. T.; Geng, T.; Akin, D.; Chang, W.-J.; Sturgis, J.; Bashir, R.; Bhunia, A. K.; Robinson, J. P.; Ladisch, M. R. *Biotechnology and bioengineering* **2003**, *81*, 618.

137. Harris, J. M. *Poly(ethylene glycol) chemistry: Biotechnical and biomedical Applications; Plenum Press: New York,* **1992**.

138. Bailey, F. E. J.; Koleske, J. Y. *Poly(ethylene oxide); Academic: New York,* **1984**.

139. Jeon, S. I.; Andrade, J. D. *J. Colloid Interf. Sci.* **1991**, *142*, 159.

140. Jeon, S. I.; Lee, J. H.; Andrade, J. D.; De Gennes, P. G. *J. Colloid Interf. Sci.***1991**, *142*, 149.

141. Gombotz, W. R.; Hoffman, A. S. *J. Biomed. Mater. Res.* **1991**, *25*, 1547.

142. Unsworth, L. D.; Sheardown, H.; Brash, J. L. *Langmuir* **2005**, *21*, 1036.

143. Palegrosdemange, C.; Simon, E. S.; Prime, K. L.; Whitesides, G. M. *J. Am. Chem. Soc.* **1991**, *113*, 12.

144. Prime, K. L.; Whitesides, G. M. *Science (Washington, DC, United States)* **1991**, *252*, 1164.

145. Prime, K. L.; Whitesides, G. M. *J. Am. Chem. Soc.* **1993**, *115*, 10714.

146. Ostuni, E.; Chapman, R. G.; Holmlin, R. E.; Takayama, S.; Whitesides, G. M. *Langmuir* **2001**, *17*, 5605.

147. Feldman, K.; Haehner, G.; Spencer, N. D.; Harder, P.; Grunze, M. *J. Am. Chem. Soc.* **1999**, *121*, 10134.

148. Pertsin, A. J.; Grunze, M. *Langmuir* **2000**, *16*, 8829.

149. Pertsin, A. J.; Hayashi, T.; Grunze, M. *J. Phys. Chem. B* **2002**, *106*, 12274.

150. Luk, Y.-Y.; Kato, M.; Mrksich, M. *Langmuir* **2000**, *16*, 9604.

151. Vanderah, D. J.; Valincius, G.; Meuse, C. W. *Langmuir* **2002**, *18*, 4674.

152. Vanderah, D. J.; La, H.; Naff, J.; Silin, V.; Rubinson, K. A. *J. Am. Chem. Soc.* **2004**, *126*, 13639.

153. Vanderah, D. J.; Arsenault, J.; La, H.; Gates, R. S.; Silin, V.; Meuse, C. W. *Langmuir* **2003**, *19*, 3752.

154. Li, L. Y.; Jiang S. Y. *J. Phys. Chem. B* **2005**, *109*, 2934.

CHAPTER 2

THEORY OF TWO-COMPONENT MIXED SAMS AND CHARACTERIZATION OF TWO-COMPONENT ORGANOTHIOL MIXED MONOLAYERS ON GOLD

2.1 Theory of two-component mixed SAM

Mixed monolayers of self-assembling molecules formed by the co-adsorption of different thiols from solutions containing a mixture of thiols have been employed and studied in many molecular-based devices and sensor.[1-21] Several mixed monolayer systems include alkanethiols with different chain lengths which can give rise to single phase or multiphase monolayers depending on the experimental conditions.[10,12,14] Other systems involve alkanethiols with different end group functionalities.[6] The structural characteristics of mixed monolayers and how they affect the phase behavior of mixed monolayers is thus very important in investigations of mixed SAMs. Mixed monolayers can be characterized using several analysis techniques .Early experiments used contact angle measurements,[22,23] ellipsometry,[24,25] polarized infrared external reflectance spectroscopy (PIERS),[13] X-ray photoelectron spectroscopy (XPS).[26,27] More recently, time-of-flight secondary ion mass spectrometry[28] and scanning tunneling microscopy (STM)[29] have been used, among others.

The formation mechanism of mixed SAMs, specifically the surface composition of the monolayers adsorbed from a solution containing two or more thiols is determined

either by the long term equilibration between the monolayers in the SAMs and the monolayer precursors in the solution (thermodynamic control), or by the kinetics of the initial adsorption step (kinetic control). The mechanism controlling the composition in the final state of the mixed monolayer is thus very complicated. Several studies on how kinetic control affects the final surface composition of mixed SAM monolayers have shown that at room temperature, the exchange between the thiolates in the SAM and in the assembly solution is slow and depends on the concentration of thiol in solution. It is also strongly influenced by defect sites within the monolayer or on the surface of the metal substrate.[6,10,30-35] Thus, for short dipping times, the SAM has not reached equilibrium and the final composition of the SAM is kinetically determined, and is dependent on the rate of adsorption of the thiol and the exposure time.

Bain and Whitesides observed that the thermodynamic control of the final composition in a SAM, particularly the preferential adsorption of longer chains over shorter chains (long chains have higher energy of adsorption but a slower rate of adsorption from solution), works in the opposite direction to the kinetic control of the adsorption process.[5] To explain this observation and determine the structure of a mixed SAM, the intermolecular interactions between nearest neighbors within the SAM must be taken into account. More recent studies reported that thermodynamic factors relative to the interactions between adsorbed nearest neighbor species are important in determining the structural characteristics of two component SAMs and provided a detailed thermodynamic analysis of phase behavior of mixed SAMs.[13,14] The experimental result[2,36] that a two component SAM eventually contains only long chain thiol adsorbate after exposure to a solution containing mixed alkanethiols with long and short chains for

a long time (~90 hours) indicates a thermodynamically controlled growth process rather than kinetic control of the adsorption process because the interactions (in this case, the van der Waals force) between long chain thiol molecules leads to a stable and well formed monolayer. This also explains the above observation that long chain thiols are always preferentially adsorbed over shorter chain thiols, as the intermolecular interactions between long chain thiols are stronger than those between short chain thiols.

In studies on the structure and phase behavior of mixed SAMs, several papers have shown that the surface composition of two components is non-linearly dependent on the relative concentrations of two components in the adsorption solution.[2-4,13] Based on Bragg-Williams solution theory,[37,38] which describes the change of state on forming mixed SAMs from solutions, Folker et al.[14] derived the thermodynamic relationship between the composition of the SAM and the composition of the adsorption solution (eq 1) to describe the behavior of a two-component SAM monolayer.

$$R_{soln} \exp(-\Delta(\Delta\mu)/kT) = (\chi_{A,SAM}/(1-\chi_{A,SAM})) \exp((\omega/kT)(1-2\chi_{A,SAM})) \quad (1)$$

$$\Delta(\Delta\mu) = \Delta\mu_A - \Delta\mu_B = (\mu_A^* - \mu_A^\dagger) - (\mu_B^* - \mu_B^\dagger) \quad (2)$$

In eqs 1 and 2, R is the ratio of the concentration of the two thiols in solution and is an experimentally controlled parameter, $\chi_{A,SAM}$ and $\chi_{B,SAM}$ are the mole fractions of component A (the long-chain alkanethiol) and component B (the short-chain alkanethiol), respectively, in the SAM monolayer and are experimentally measured parameters, ω is the interaction parameter, k is Boltzmann's constant, T is the absolute temperature of the system, μ^* is the chemical potential of the thiolate in the single-component SAM, $\mu^\dagger$ is the chemical potential of the thiol when it is at infinite dilution (the mole fraction of thiol in solution $\rightarrow 0$) and the two unknowns are $\Delta(\Delta\mu)$ and ω. $\Delta(\Delta\mu)$ is independent of the

interaction parameter and is only dependent on the standard-state chemical potentials of the adsorbed species in the solution and in the monolayer. The interaction parameter term, ω, describes the intermolecular interaction between the adsorbed species and is derived from the change in internal energy that occur on going from two separate, single-component monolayers- that is, the reference state (see Fig. 2.1) to a mixed monolayer. The value of the interaction parameter in units of *k*T will determine the phase behavior of the SAMs. For simplicity, eq. 1 can be rewritten as eq. 3,

$$\chi_{A,soln}\left[(\chi_{A,SAM}/(1-\chi_{A,SAM}))\exp((\omega/kT)(1-2\chi_{A,SAM})) + \exp(-\Delta(\Delta\mu)/kT)\right] = (\chi_{A,SAM}/(1-\chi_{A,SAM}))\exp((\omega/kT)(1-2\chi_{A,SAM})) \quad (3)$$

where $\chi_{A,soln}$ is the mole fraction of component A in the assembly solution. The theoretical relationships between the mole fraction of component A in the SAM ($\chi_{A,SAM}$) and the mole fraction of component A in the solution ($\chi_{A,soln}$) determined using eq. 3 are shown in Fig. 2.2.To simplify these calculations, $\Delta(\Delta\mu)$ is assumed to equal zero ($\Delta\mu_A = \Delta\mu_B$). The relationships vary in different regions of the interaction parameter. (1) When $\omega<0$, the interactions between unlike molecules are more energetically favorable than interactions between like molecules (for example, the two components of the mixed monolayer may contain electron-donor and electron-acceptor groups). (2) When $\omega=0$, then the adsorbed molecules are non-interacting, the mixture is ideal and the components are equivalent. The thermodynamic relationship is an ideal Langmuir adsorption isotherm and the surface composition of the SAM is linearly dependent on the relative composition of the adsorption solution. (3) When $0<\omega<2kT$, the components prefer to be surrounded by like molecules and complete mixing is expected. (4) If $\omega= 2kT$, a critical mixing of the two components exists in the SAM. (5) When $\omega>2kT$, three possible values of $\chi_{A,SAM}$ for

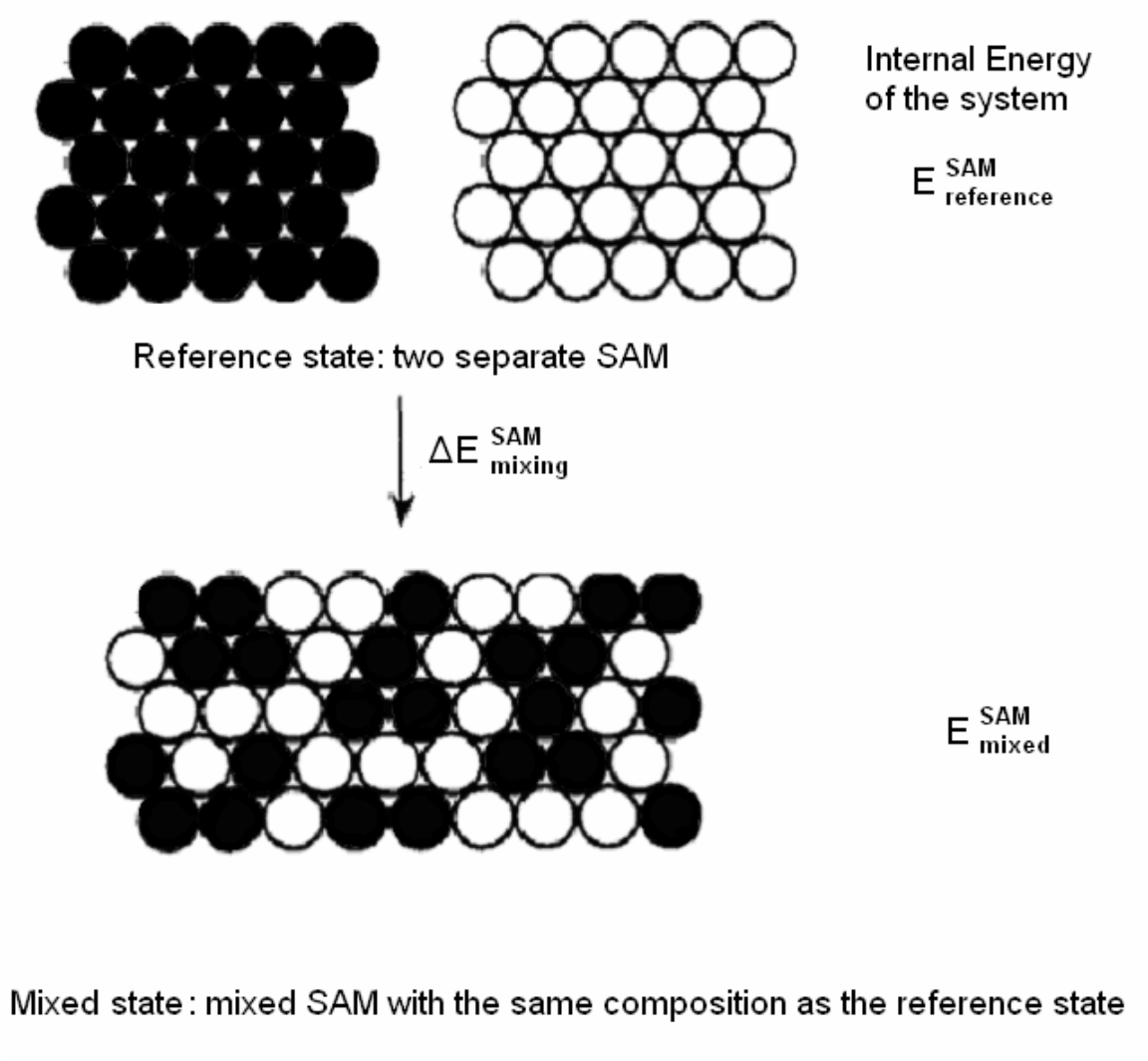

Fig. 2.1 Schematic presentation of the reference and mixed states used to derive the interaction parameter, ω.

each value of $\chi_{A,soln}$ exist over a range of values of $\chi_{A,soln}$ centered about the midpoint. By measuring which $\chi_{A,SAM}$ has the lowest free energy and selecting the candidate value of $\chi_{A,SAM}$ to have the lowest free energy for each value of $\chi_{A,soln}$, it is possible to predict that the equilibrium relationship between $\chi_{A,soln}$ and $\chi_{A,SAM}$ which corresponds to the minimum energy phases (the solid line in Figure 2.2 for $\omega = 3kT$) will be a vertical discontinuity of the adsorption isotherm that breaks vertically at the midpoint. The other two compositions (the dashed curve in Fig 2.2) correspond to the metastable phase, which will not occur at equilibrium. Once the SAM has reached equilibrium (thermodynamic control) for a solution containing an excess of the two thiols, it generally contains a single phase, which may include either a single alkanethiolate or a homogeneous mixture of both alkanethiolates, but will not consist of regions of different phases. Folker et al.[14] also stated that if the SAM film has not reached equilibrium (kinetic control) any phase segregation is due to kinetically-trapped structures in the monolayer and the SAM may include two phase. The composition of one phase could be the composition obtained at equilibrium, while the composition of the other could be haphazard, but would probably be closer to the initial, kinetically formed composition. As a SAM approaches to equilibrium, islands of the equilibrium composition will grow until the SAM reaches equilibrium. At the equilibrium point, the SAM generally is a single phase, and the single phase composition may contain either a single alkanethiolate (if there is a large difference between $\Delta\mu_A$ and $\Delta\mu_B$) or a homogenous mixture of both alkanethiolates.

The thermodynamic relationship equation can also be used to determine the mole fraction of component A in a SAM ($\chi_{A,SAM}$) as a function of the mole fraction of

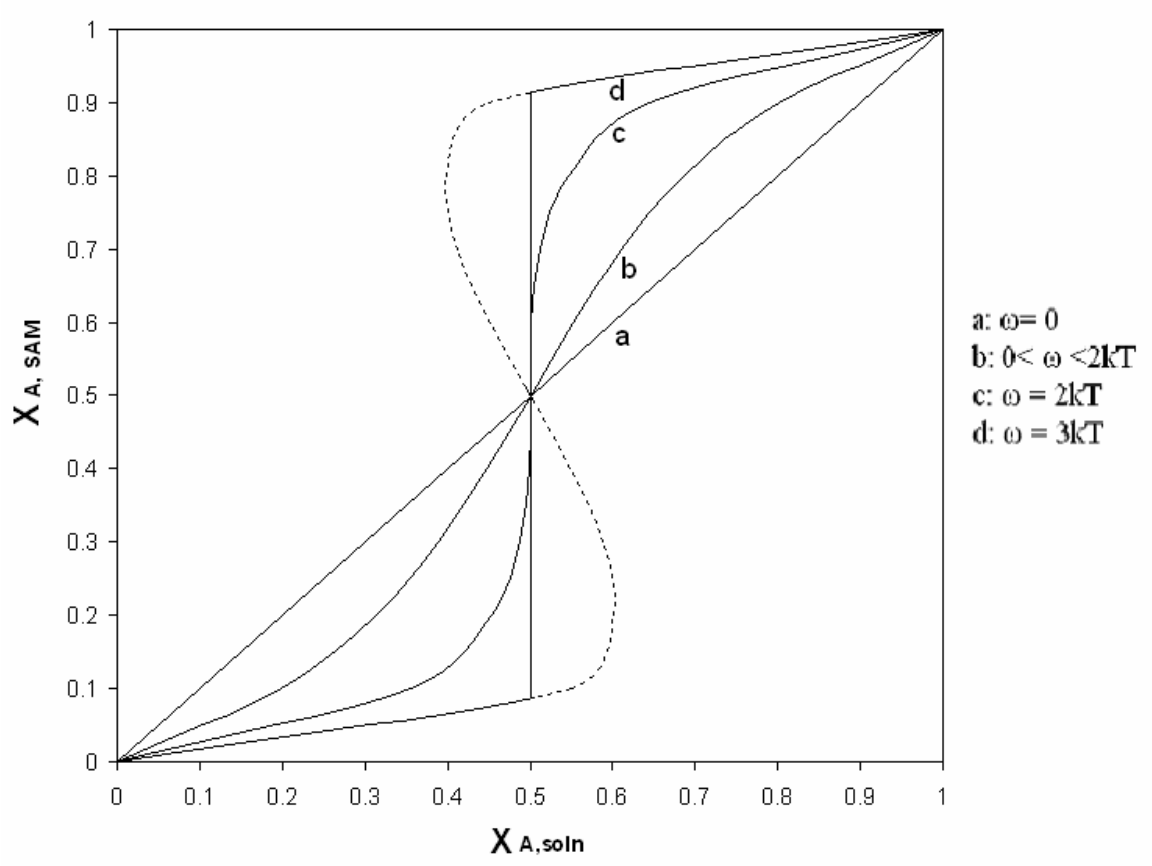

Fig. 2.2. Theoretical relationships between $\chi_{A,slon}$ and $\chi_{A,SAM}$ determined using eq. 3 and assuming $\Delta(\Delta\mu) = 0$. (a) $\omega = 0$, well-mixed SAMs (b) $0 < \omega < 2kT$ (c) $\omega = 2kT$, critical mixing SAM (d) $\omega = 3kT$, SAM in which mixing of the components is not favored.

component A in the assembly solution ($\chi_{A,soln}$) with different values of $\Delta(\Delta\mu)$ and ω (Fig. 2.3). When $\omega = 0$, the adsorption curves are Langmiur adsorption isotherms, with no interaction between adsorbed species. Curve 1 is an ideal Langmiur isotherm and $\Delta(\Delta\mu)$ equals zero, so $\Delta\mu_A = \Delta\mu_B$ and the adsorption tendency of thiol A is same with its of thiol B. For curve 2, $\Delta(\Delta\mu)$ is more than zero, so $\Delta\mu_A > \Delta\mu_B$ and the adsorption tendency of thiol A is weaker than that of thiol B. In curve 3, $\Delta(\Delta\mu)$ is less than zero so $\Delta\mu_A < \Delta\mu_B$ and the adsorption tendency of thiol A is stronger than that of thiol B. Thus, the larger $\Delta\mu_A$ is, the weaker the adsorption tendency. When $\omega < 0$ and $0<\omega < 2kT$, the adsorption curves differ but not markedly. However, for the case of ω equal to or more than 2kT, the adsorption isotherms are complicated and not applicable to the current study and will not be discussed further.

Based on these studies, for mixed SAMs assembled by the co-adsorption of different thiols from solutions containing a mixture of thiols, once the SAM has reached equilibrium, the composition of the mixed SAM monolayer is primarily determined by thermodynamic factors given sufficiently long immersion time. The equilibrium time required may be several days. However, if the SAM has not reached equilibrium, or the adsorbed species are very strongly bound and cannot be displaced easily, the kinetics may play a role in determining the composition of the mixed SAM. For example, once the pure MUA monolayer is fully formed and densely packed, the composition of a pure MUA monolayer only changes by ~20% when exposed to DDT assembly solution for 6 days.[39]

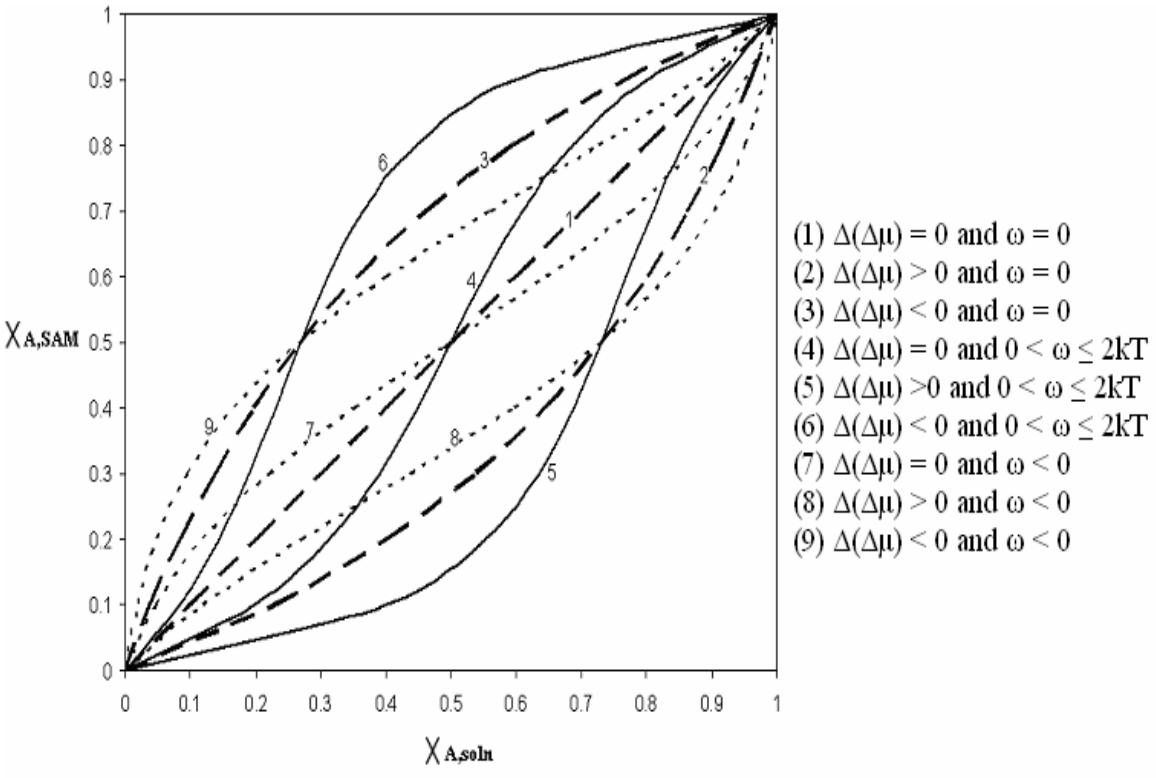

Fig. 2.3. The thermodynamic relationships between $\chi_{A,soln}$ and $\chi_{A,SAM}$ (calculated from eq. 3.) for different values of ω and Δ(Δμ).

2.2 Characterization of two-component mixed monolayers on gold

2.2.1 Introduction

In previous studies of the composition of a mixed SAM, contact angle, XPS, ellipsometry, STM, electrochemical impedance spectroscopy (EIS), auger electron and FTIR spectroscopy have been used. Here we study the characterization of two-component SAMs on gold were studied utilizing three techniques. First, the capacitance determined by cyclic voltammetry was used to measure the composition of mixed monolayers of alkanethiol and 1-mercapto-3,6,9,12-tetraoxotridecane (EG_4-SH) based on differences in the thickness and dielectric constant of the alkanethiols and EG_4-SH monolayers. Second, coulometry was used method to study composition of mixed monolayers of 4-ATP and decanethiol (DT). Because 4-ATP can be easily oxidized electrochemically and decanethiol is a non-electroactive thiol, the oxidative electrochemistry of 4-ATP was used to determine the mole fraction of 4-ATP in a mixed monolayer. Finally, surface-enhanced Raman spectroscopy (SERS) was used to obtain vibrational spectra of SAMs on roughened gold surfaces and characterize mixed SAM monolayers of EG_4-SH/ATP.

2.2.2 Experimental

Chemicals. All alkanethiols (hexanethiol (C6), decanethiol (C10), octadecanethiol (C18)) were purchased from Aldrich Chemical Co. 4- aminophenol thiol (Aldrich) was recrystallized two to three times from methanol (Fisher) and stored in the dark at 0℃. 1-mercapto-3,6,9,12-tetraoxotridecane (EG_4-SH)was synthesized by following a general procedure. Structural assignments were made from proton nuclear magnetic resonance data. Sample purity was determined from high resolution gas chromatography/mass

spectrometry analysis. Ethanol (190 proof, Florida Distillers), $NaClO_4$ and 70% $HClO_4$ (Fischer) were used as received.

SAM preparation. Before each surface modification, gold foil (99.999% purity, Alfa) was repeatedly cleaned with piranha solution (1: 3 H_2O_2:H_2SO_4), and 18 MΩ Millipore filter water (Millipore H_2O). The monolayers were prepared by immediately immersing the gold substrates in 1.0×10^{-3} mol/L solutions of the corresponding thiol in 95% ethanol for 24 hr. Upon removal from the thiol solution, the SAMs were rinsed with ethanol and dried with nitrogen.

Electrochemistry. All electrochemistry experiments were performed in a homemade Teflon cell using an EG & G Princeton Applied Research potentiostat model 273 with HP 7015B X-Y recorder. A standard three-electrode system was used in which a Pt wire was the counter electrode, Ag/AgCl was the reference electrode and the gold foil modified with SAM monolayer was the working electrode. The real gold electrode surface area exposed to solution was measured by cyclic voltammetry using 0.1 M ferricyanide in 0.1M KCl electrolyte solution[40]. The scanning rate was 100mV/s. In the capacitance measurements, the capacitive current densities data were obtained from Au electrode modified with SAM monolayer in 0.1M $NaClO_4$ solution. In the coulometric experiments, the surface composition of 4-ATP in a mixed SAM was measured by stepping the electrode potential through a one-electron oxidation wave of 4-ATP in 1M $HClO_4$ electrolyte solution.

Surface-enhanced Raman spectroscopy. The SAM monolayer was immobilized on a roughened gold surface. The gold electrode was electrochemically roughened in 0.1 M KCl by 20 oxidation-reduction cycles from -300 mV to 1200 mV at the rate of

500mV/s. A 30 s hold was used on the negative end of the cycles, and a 2s hold at the positive end. The electrode was then removed from the KCl solution and thoroughly rinsed with distilled deionized water to remove any chloride ions. The SAM surfaces were characterized using a home made Raman spectrometer equipped with a HeNe Laser (632.5 nm) and an Ocean Optics HR2000 spectrometer.

2.2.3 Results and Discussion

Characterization of mixed SAM containing EG_4-SH and alkanethiol with different chain lengths by capacitance measurement. Here, the capacitance measured by cyclic voltammetry was used to determine the relationship between the composition of two-component SAMs and the composition of the assembly solution. After the gold electrode has been modified with a SAM monolayer, the high insulating properties of the SAM layer prevented electrons from reaching the gold surface. According to the electrostatic model, a charged surface and electrolyte solution interface can be viewed as capacitors, allowing the capacitance measurement to be used here to study the surface composition of the mixed SAM monolayer. Fig. 2.4 presents the capacitive current densities of SAMs of DT and EG_4-SH individually on Au electrodes. The capacitive current densities of EG_4-SH were much higher than for DT. By using eq. 4, the capacitance of DT and EG_4-SH were calculated.

$$I=2\times C\times \upsilon \qquad (4)$$

where I is the capacitive current density of the SAM obtained from CV measurement, C is the capacitance of the SAM monolayer and υ is the scan rate. The results revealed that the capacitance of EG is much higher than that of DT. The difference in capacitance is a

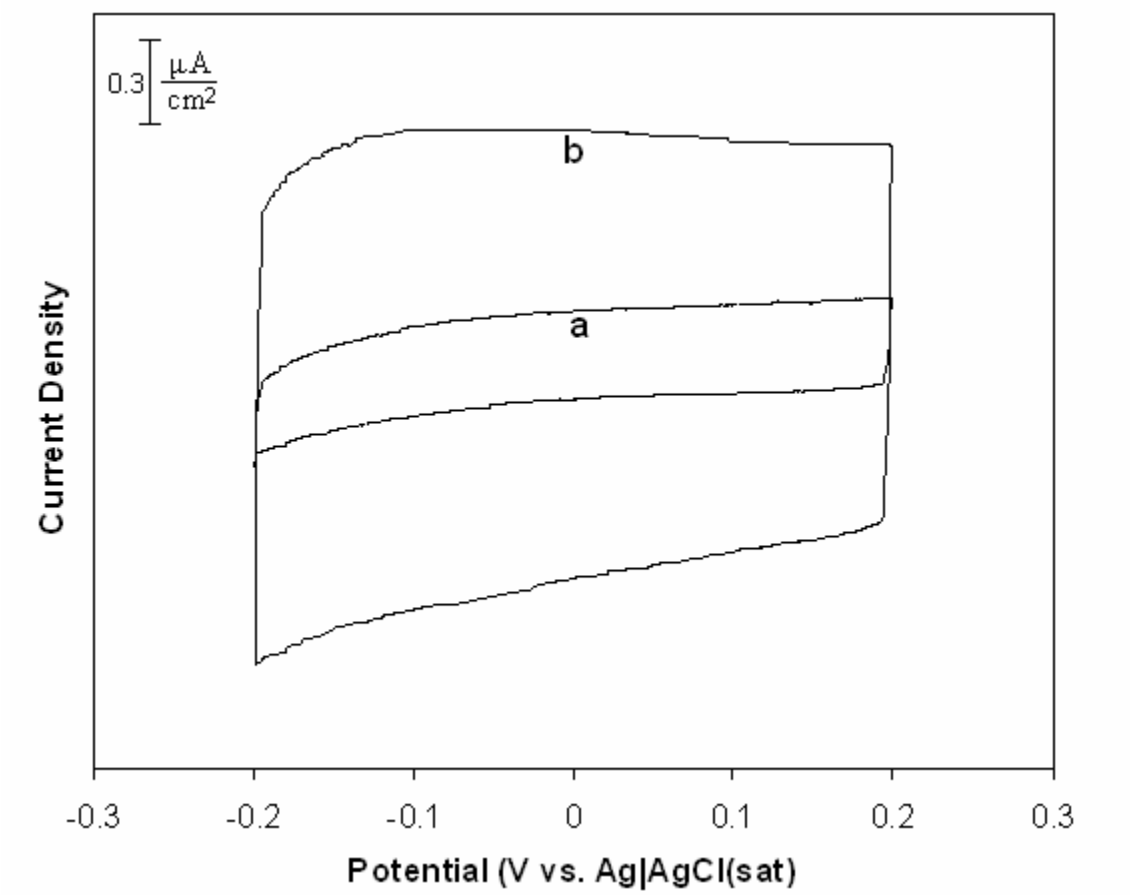

Fig. 2.4 Capacitive current densities of SAMs of (a) DT and (b) EG_4-SH individually on Au electrodes in 0.1M $NaClO_4$ at a scan rate of 100mV/s.

characteristic of the organic adsorption due to the difference in the dielectric constant and the thicknesses of the two materials (eq. 5).

$$C = \varepsilon \bullet A / d = K \bullet \varepsilon_o \bullet A / d \quad (5)$$

where A is the area of the gold electrode, a constant here, d is the distance between the plates, ε is the relative permittivity, ε_o is the permittivity of free space (vacuum permittivity) and K is the dielectric constant of the insulating medium, which describes the ability of the dielectric to store electrical energy.

A series of CV measurements were achieved with mixed SAM monolayers assembled from adsorption solutions containing EG_4-SH and alkanethiol with different chain lengths over a range of molar ratios. The plot of total capacitances vs. the mole fraction of EG_4-SH in the adsorption solution ($\chi_{A,SAM}$) is presented in Fig. 2.6. The alkanethiol in the mixed SAM of curve 1 is hexanethiol, which has six carbons in its hydrocarbon chain. The alkanethiol in curve 2 is decanethiol, which has ten carbons, and curve 3 is octdecanethiol, with eighteen carbons. The results show that at $\chi_{A,SAM} = 0$, which is pure alkanethiol without EG_4-SH, as the chain length of alkanethiol increases, the value of the capacitance of the alkanethiol decreases. This is because when the chain length of the alkanethiol increases, the thickness of the SAM also increases. According to the capacitance formula (eq 5.), the capacitance of SAM is expected to decreas. The relationship between the capacitances of pure alkanethiol monolayer and the thickness of the alkanethiols (C_6, C_{10} and C_{18}) is summarized in Table 2.1 and clearly demonstrates that as the thickness of the alkanethiol (chain length) increases, the capacitance of the alkanethiol monolayer decreases. The other observation that can be made from Fig. 2.5 is

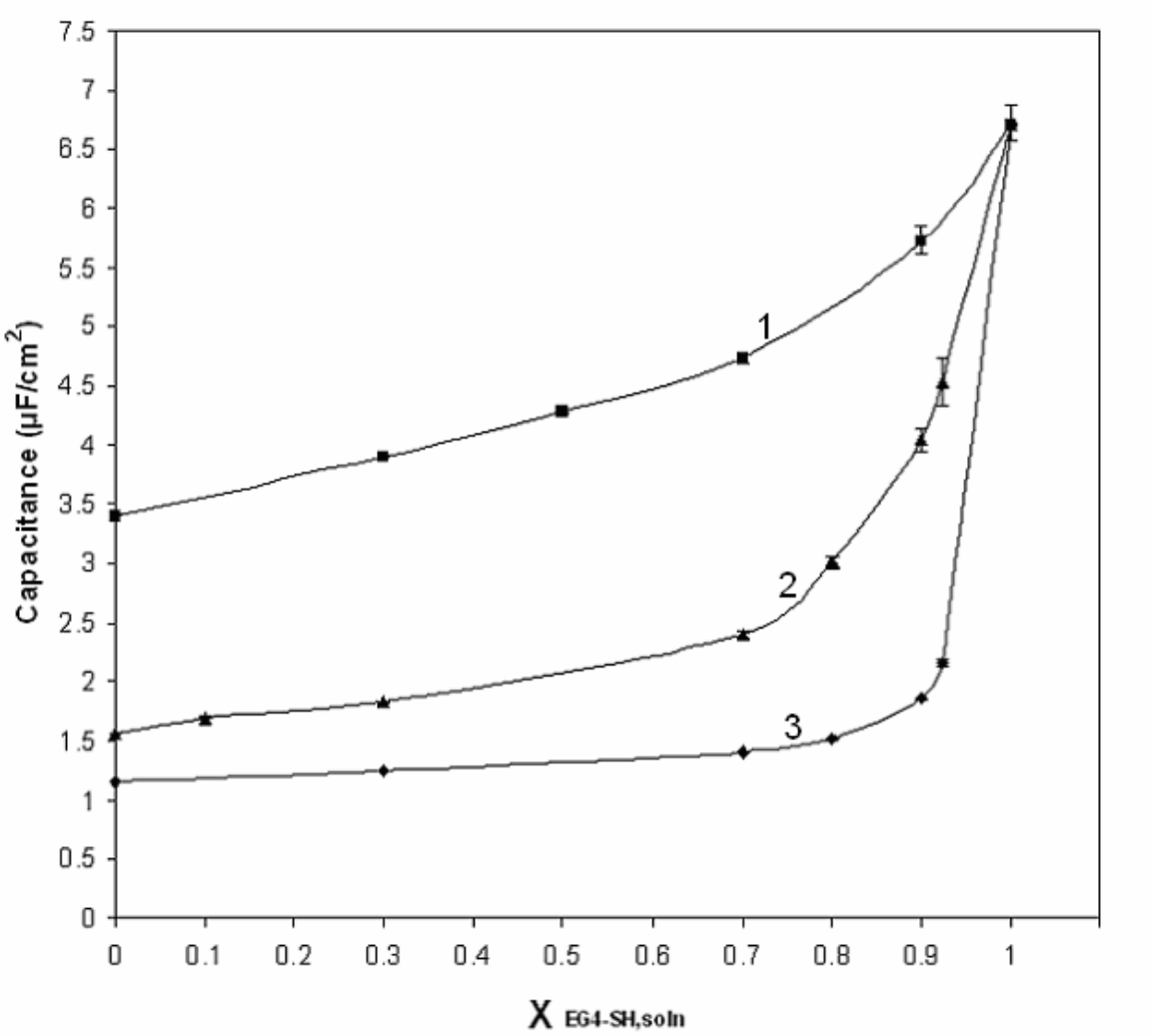

Fig 2.5. Plot of capacitance vs. the mole fraction of EG_4-SH in an adsorption solution of EG_4-SH /alkanethiol with different chain lengths. (■) hexanethiol (▲) decanethiol (♦) octdecanethiol

that as the mole fraction of EG_4-SH in the adsorption solution increases, for all three curves the capacitance of the corresponding SAM increases.

Table 2.1 Relationships between capacitance and thickness

the numbers of carbons	thickness of alkanethiol (nm)	Capacitance ($\mu F/cm^2$)
6	0.8	3.4
10	1.45	1.56
18	2.4	1.15

Several electrochemical studies of mixed thiol monolayers on gold have indicated that from a macroscopic viewpoint, each component of the binary mixed SAM can be assumed to act as an individual capacitor in parallel. Here the difference in the total capacitance of two capacitors between a parallel connection and in series connection will be discussed first. The capacitance C of a capacitor is its ability to store an electrical charge and is the proportionality coefficient between the charge Q on the capacitor and the applied voltage V. If two capacitors with capacitance C_1 and C_2 are connected in parallel (see Fig.2.6a), they take the total charge Q_T, which is the sum of the individual charges (Q_1 and Q_2). Because the voltage V applied to both capacitors is the same, the capacitance of the parallel connection is

$$C_T = C_1 + C_2 \quad (6)$$

If the two capacitors are series-connected (see Fig. 2.6b), both capacitors take the same charge. The value of the total charge (Q_T) is equal to one of the individual charges and the applied voltage is the sum of the individual voltages. So, the capacitance of the series connection fulfills the equation.

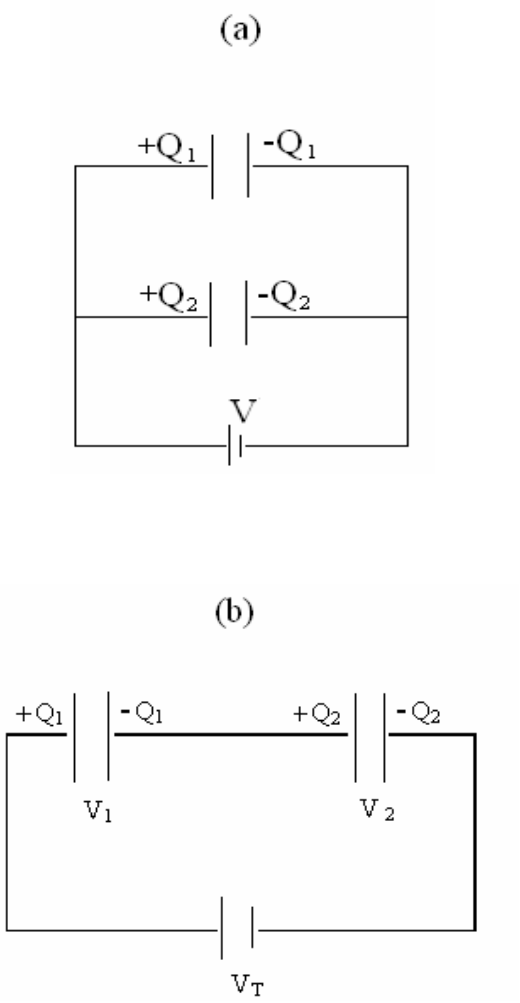

Fig. 2.6 Schematic representations of two capacitors connected (a) in parallel and (b) in series.

$$1/C_T = 1/C_1 + 1/C_2 \quad (7)$$

The capacitance of each capacitor (C_1 and C_2) in turn consists of the capacitances C_A and C_B representing the values for a pure SAM of either component A or B, respectively, and the mole fraction of the component A or B in the monolayer. Because each component of a two-component SAM is assumed to act as a capacitor in parallel, the total capacitance of a mixed monolayer measured in the CV experiment is

$$C_T = \chi C_A + (1-\chi) C_B \quad (8)$$

where the total capacitance (C_T) is the sum of the capacitances of the individual component capacitors weighted by their mole fraction. Here, component A is EG_4-SH, and B is alkanethiol. χ is the mole fraction of component A (EG_4-SH) in the monolayer. C_A and C_B are the capacitances of the single component A and B, respectively. This equation can be used to convert the capacitance data (Fig. 2.5) for a binary mixed SAM consisting of two components into the surface composition of a mixed SAM (χ) by determining the capacitance of the mixed SAM (C_T) when the capacitances of both single component SAMs (C_A and C_B) are known[39]. Defects in the monolayer are assumed to have only a negligible effect on the capacitance of a well made SAM, and the diffuse layer capacitance can be neglected for a gold electrode modified with thiol SAM at the relatively high electrolyte concentrations used in this study[25,41] The mole fraction of EG_4-SH in a SAM monolayer on gold ($\chi_{A,SAM}$), which is calculated from eq. 8 and re-plotted, as a function of the mole fraction of EG_4-SH in solution ($\chi_{A,soln}$) is shown in Fig. 2.7. The results show that for all three adsorption isotherms, the mole fraction of EG_4-SH in the SAM is lower than the corresponding mole fraction of EG_4-SH in the adsorption solution, especially when the mole fraction of EG_4-SH in the SAM is below

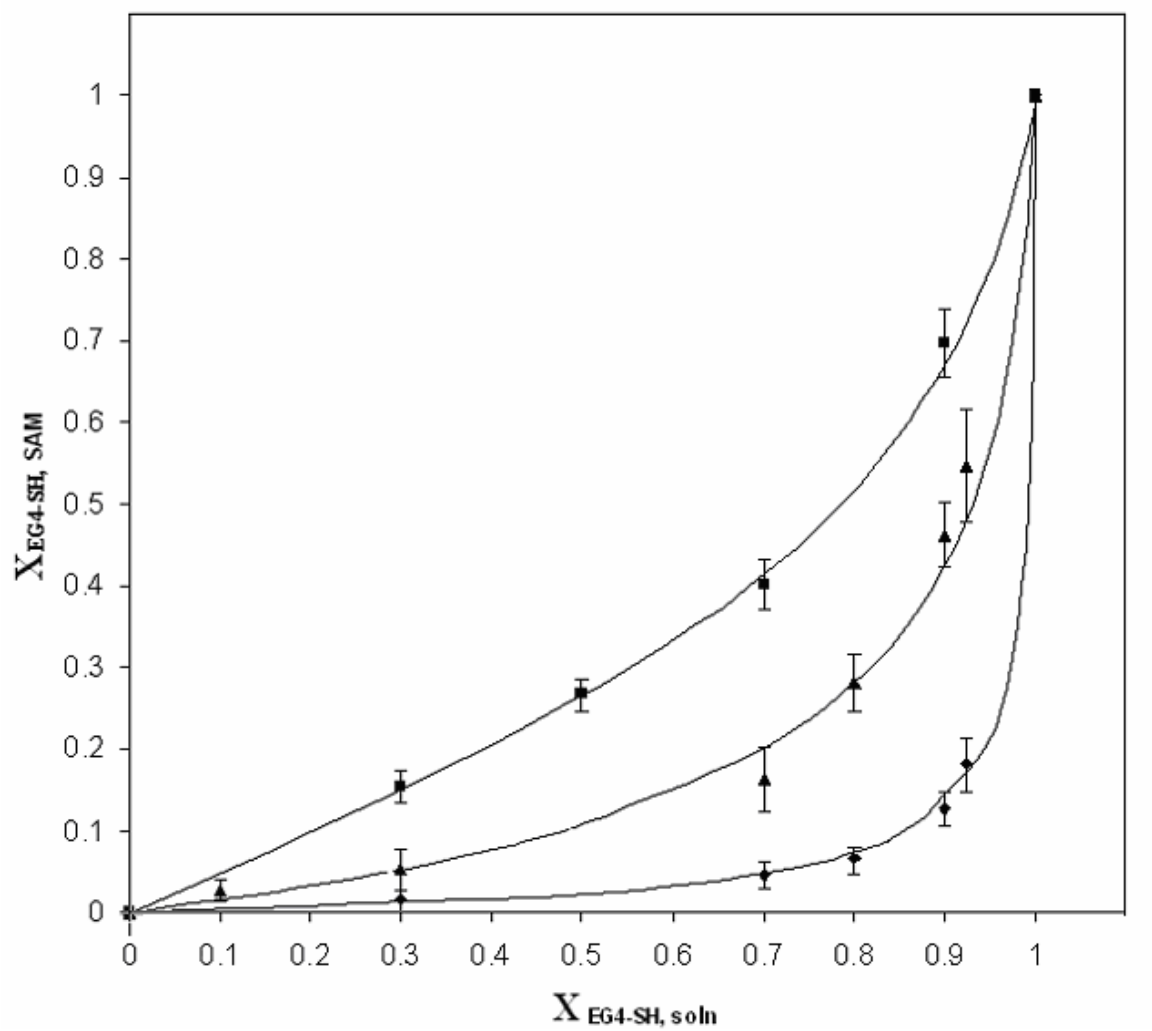

Fig. 2.7. Adsorption isotherms for EG_4-SH/alkanehtiol mixed monolayers. The mole fraction of component A (EG_4-SH) in a mixed SAM of EG_4-SH /alkanethiol (calculated from the measured capacitance of Fig. 2.6) *vs.* the mole fraction of EG_4-SH in adsorption solution. (■) hexanethiol/EG_4-SH, (♦) decanethiol/EG_4-SH, (●) octdecanethiol/EG_4-SH.

0.7. This indicates that hexanethiol, decanethiol and octdecanethiol molecules have a stronger tendency to adsorb on gold surface than the EG_4-SH molecules. The reason could be that EG_4-SH has a higher solubility in ethanol due to its greater affinity towards the (polar) ethanol and thus a poorer tendency to adsorb onto the gold substrate. Fig. 2.7 also shows that for a specific mole fraction of EG_4-SH in the assembly solution, for example at 0.7, as the chain length of the alkanethiol increases, the mole fraction of the EG_4-SH in the SAM decreases. This means for alkanethiol, longer chain lengths will have a stronger tendency to adsorb on gold surface compared to EG_4-SH. An earlier study on mixed SAMs of EG_4-SH and alkanethiol demonstrated that after 24 hours dipping time, the SAM has reached equilibrium, so here three mixed SAM systems of EG_4-SH/alkanethiol with different chain lengths were studied, and eqs. 3 and OriginPro7.5 were applied to obtain the values of thermodynamic factors which are shown in Table 2.2.

Table 2.2. Values of ω and Δ(Δμ) for mixed SAMs

Type of mixed SAMs	ω/*k*T	Δ(Δμ)/*k*T
EG_4-SH /hexanethiol	-0.59686	1.30
EG_4-SH /dexanethiol	-0.61333	2.60
EG_4-SH/octdecanethiol	-1.1512	4.90

In these three mixed SAM systems, the values of ω are all less than zero. This indicates that the interactions between EG_4-SH and alkanethiol are more energetically favorable than interactions between EG_4-SH and EG_4-SH or alkanethiol and alkanethiol. As the chain length of the alkanethiol increases, ω becomes more negative, which means

the interactions between EG_4-SH and alkanethiol becomes stronger. The value of $\Delta(\Delta\mu)$ shows that $\Delta\mu$ (EG_4-SH)> $\Delta\mu$ (hexanethiol)> $\Delta\mu$ (decanethiol)> $\Delta\mu$ (octdecanethiol). Due to their smaller $\Delta\mu$, which implies a stronger adsorption tendency, the octdecanethiol molecules have strongest tendency to adsorb onto a gold surface compared to EG_4-SH, hexanethiol and decanethiol, which is in good agreement with previous studies[2,4,5,15].

Characterization of 4-ATP/DT mixed monolayer by coulometry measurements and capacitance. Here, the mole fraction of 4-ATP in a mixed monolayer as a function of mole fraction of 4-ATP in the adsorption solution was determined by coulometry measurements based on the electroactivity of the adsorbed 4-ATP species. A series of cyclic voltammetry scans were conducted for mixed SAMs formed by adsorption from solutions composed of DT and ATP mixtures with various mole fractions, in 1M $HClO_4$ electrolyte. Comparing this series of CV data with cyclic voltammetry results for a pure 4-ATP monolayer (Fig. 2.8) revealed, similar surface confined waves and the average peak position, E°, did not shift as a function of the mole fraction of 4-ATP in the adsorption solution. As the mole fraction of 4-ATP in the solution decreased, the oxidative current density decreased. This result indicates that DT is not electrochemically active and only acts to dilute the concentration of electroactive 4-ATP. This agrees with the results of an earlier electrochemistry study of a 4-ATP/ODT mixed monolayer system.[42] In cyclic voltammograms of 4-ATP (Fig. 2.8), an irreversible oxidative wave was observed at approximately 0.80 V (peak A), corresponding to one electron oxidation process of 4-ATP. Here the electrode potential was stepped from 0.65 V to 0.90 V to give the current densities of this peak for the various mole fractions of

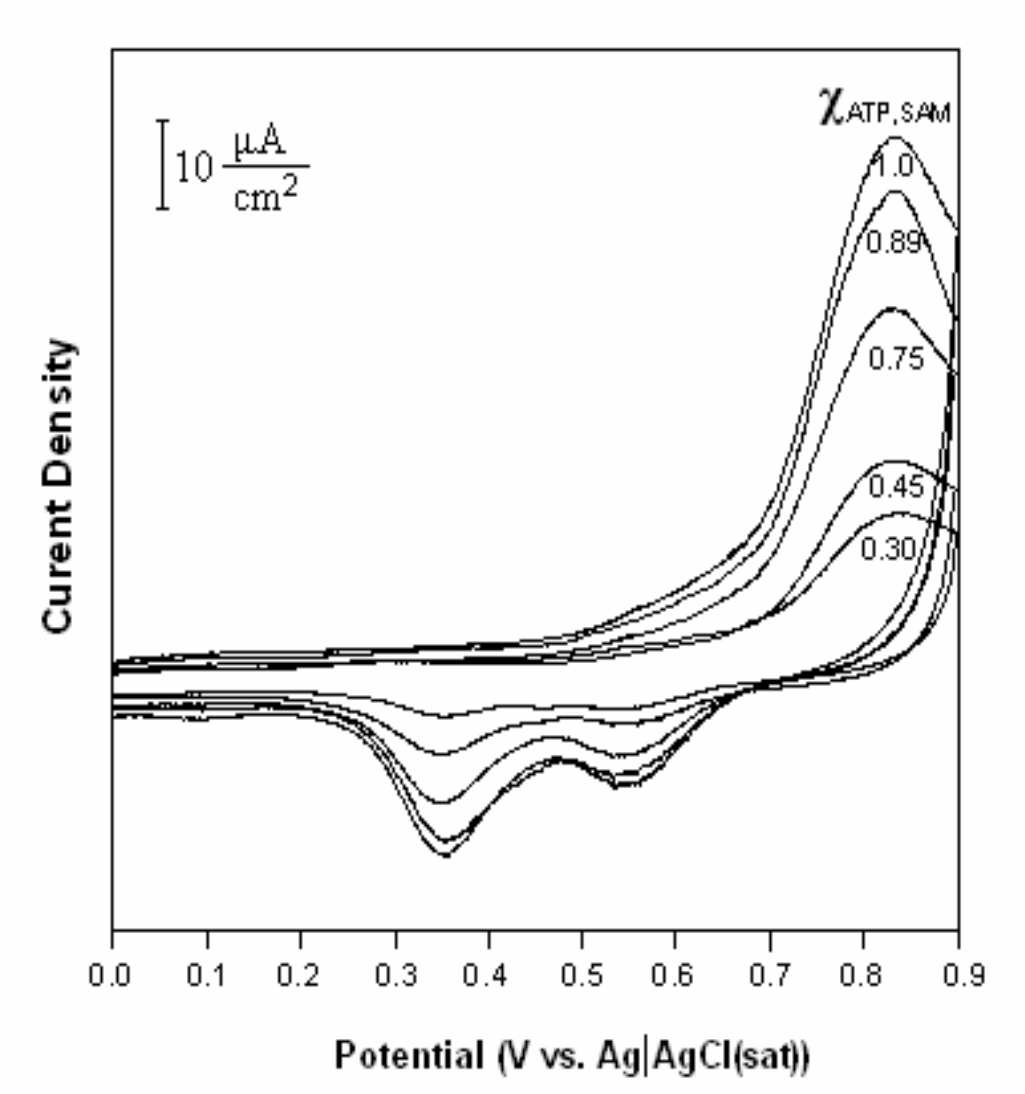

Fig. 2.8 Voltammetric behavior of a 4-aminothiophenol (4-ATP)/decanethiol (DT) mixed monolayers on Au electrode immersed in 0.1 M HClO4 solution as a function of 4-ATP mole fraction. The scan rate was 100 mV/s

4-ATP in the assembly solutions. Thus, the amount of 4-ATP in the SAM monolayer with its various mole fractions can be measured by Faraday's Law, namely the amount of current is proportional to the amount of species oxidized or reduced, and the adsorption isotherm for ATP/DT mixed monolayer is plotted and shown in Fig. 2.9. The relationship between the mole fraction of 4-ATP in the mixed monolayer and the mole fraction of4-ATP in the solution is not linear, with a sharp break occurring as the mole fraction of 4-ATP in adsorption solution reaches 0.70. The adsorption isotherm shows a lower mole fraction of 4-ATP in the SAM, when the mole fraction of 4-ATP in the adsorption solution is below 0.7. This indicates the adsorption of decanethiol on gold is more favorable than 4-ATP in the assembly ethanol solution, which agrees with the previous findings[43], and the rate of adsorption of DT is bigger than the rate of adsorption of 4-ATP. One reason for this could be that the presence of an amino group results in 4-ATP having a greater affinity towards the (polar) ethanol, a higher solubility in ethanol and thus a poorer tendency to come out of the solution and adsorb onto the gold surface. Alternatively, this could be due to the thermodynamic mechanism of SAM formation, where the longer chain length decanethiol is thermodynamically more stable than 4-ATP, with its short chain length, due to the van der Waals forces between longer chain length decanethiol molecules being stronger than that in the 4-ATP molecules. It is also possible that as the mole fraction of ATP exceeds 0.8, more ATP is adsorbed onto the surface. It suggests that in this mixed SAM system, when a large amount of ATP is adsorbed on the surface the highly ordered SAM monolayer becomes disordered.

Here, the 4-ATP and DT mixed monolayer system was also studied using a capacitance technique, but the adsorption isotherms determined by these two techniques

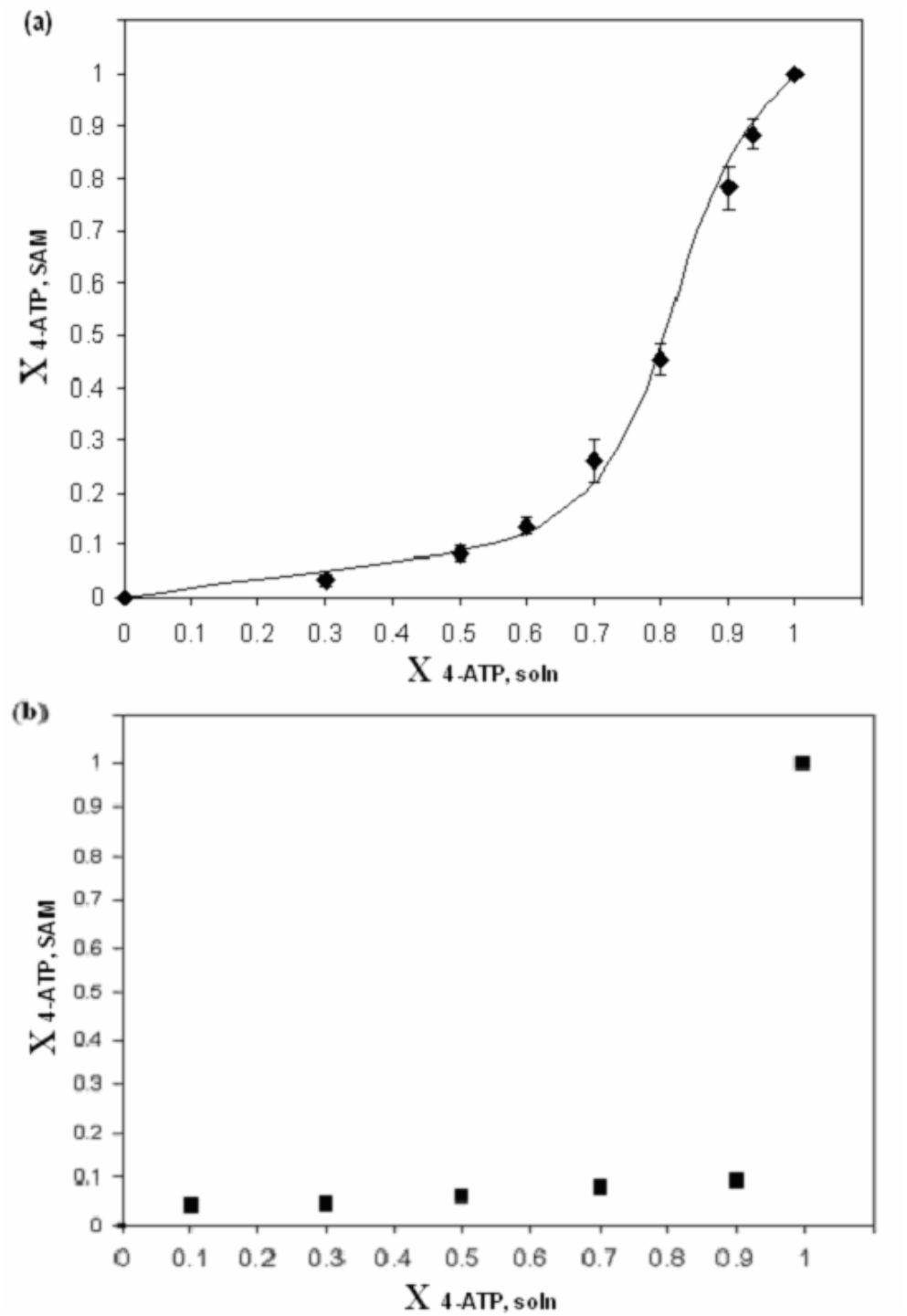

Fig. 2.9 (a) Adsorption isotherm for 4-aminothiolphenol/decanethiol mixed monolayers determined by coulometry. (b) Adsorption isotherm for 4-aminothiolphenol/decanethiol mixed monolayers determined by capacitance.

were completely different and the data provided by the capacitance measurement was of very poor quality. One reason for this could be that the capacitance measurement was not suitable for use in the SAM systems which include a 4-ATP monolayer. When the composition of a mixed monolayer of EG_4-SH and DT was determined by the capacitance technique, defects in the SAM monolayer were assumed to have only a negligible effect on the capacitance of a well-ordered SAM. For a mixed monolayer film with a low mole fraction of 4-ATP, the surface of 4ATP and DT is still well-ordered, but as the mole fraction of 4-ATP increases, the mixed monolayer becomes more and more disordered and many defects are present. The capacitance of a mixed monolayer with a high concentration of 4-ATP will be seriously affected by the defects on the SAM monolayer, so the capacitance technique is not suitable for use in determining the composition of mixed monolayers which contain 4-ATP. Also 4-ATP is an electroactive compound, electrons can reach the gold surface from the electrolyte solution and thus increase the capacitance values of SAM monolayer containing 4-ATP, skewing the results.

Characterization of mixed SAMs of 4-ATPG_4-SH by SERS and coulometry measurement. The surface-enhanced Raman spectroscopy technique was used here to obtain vibrational spectra of SAM on a roughened Au surface to measure the composition of EG_4-SH in a mixed SAM monolayer as a function of the mole fraction of EG_4-SH in the adsorption solution. The Raman spectrum obtained from the pure OEG-SAM stretching band at 2921 cm^{-1}, the CH_2 antisymmetrical stretching band at 2963 cm^{-1} and the CH_3 antisymmetrical stretching band at 2999 cm^{-1} were observed and are clearly

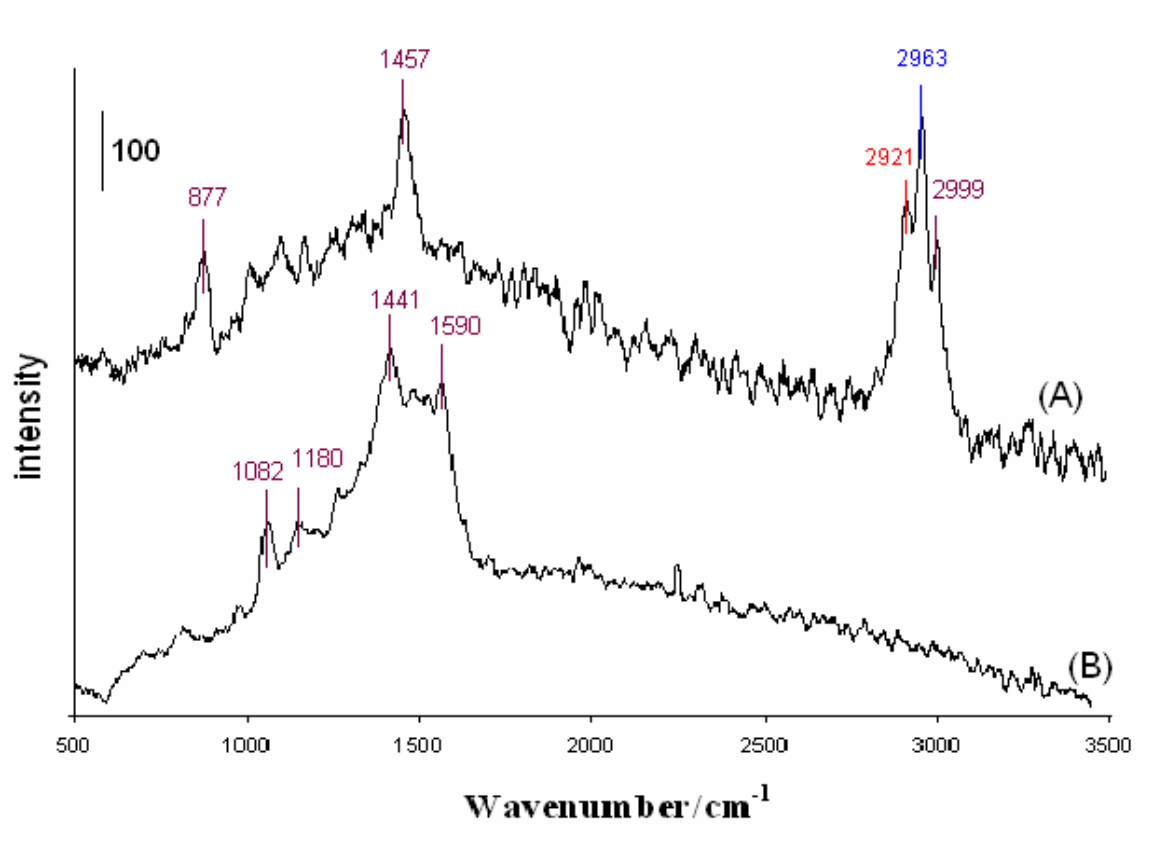

Fig. 2.10 Raman spectra of EG_4-SH (A) and 4-ATP (B) from 500 to 3500cm^{-1}.

present in Fig. 2.10.a, in agreement with results reported by Kozielski and Vanderah et al. [44-46]. Figure 2.10.b shows the Raman spectrum of pure ATP-SAM. A strong band is visible at 1082 cm^{-1}, which is assigned to C(benzene ring)-S stretching vibration. The relational band at 1590 cm^{-1} is assigned to the C-C stretching vibration of the benzene rings. A weaker band for the roughened Au surface was recorded in the spectral range from 500 to 3500 cm^{-1}.The CH_2 rocking band is at 877 cm^{-1}, the CH_2 scissoring band is at 1457 cm^{-1}, and the CH_2 symmetrical band at 1180 cm^{-1} is corresponds to the C-H bending vibration, while the 1441 cm^{-1} band corresponds to a combination of the C-C stretching and C-H bending vibrations. Due to the detection limit, no band was observed in the spectral range from 2500 to 3500 cm^{-1}. As the adsorption solution was diluted by adding 4-ATP, the intensities of the three Raman spectrum peaks at 2921, 2963 and 2999 cm^{-1} decreased. The amount of EG_4-SH adsorbed on the Au surface can thus be determined by counting the total intensities of these three SERS spectra band as a function of mole fraction of the EG_4-SH in the adsorption solution.

This SAM system was also examined using coulometry measurements. In coulometry measurement experiments, the mole fraction of 4-ATP in the mixed monolayer as a function of mole fraction can be coulometrically determined due to the electroactivity of the adsorbed 4-ATP species and the nonelectroactivity of the EG_4-SH species. The relationships between the mole fraction of 4-ATP in a mixed SAM and the mole fraction of 4-ATP in a mixed thiol solution are determined by SERS techniques and coulometry measurements and are presented in Fig 2.11. The data from both techniques show good agreement with each other. The results show that when the mole fraction of 4-ATP in the adsorption solution is below 0.3, 4-ATP has a stronger tendency to adsorb

onto gold than EG_4-SH. This indicates that the rate of adsorption of 4-ATP is higher than the rate of adsorption of EG_4-SH. Above 0.3, the difference between the adsorption tendencies of the two thiols decreases.

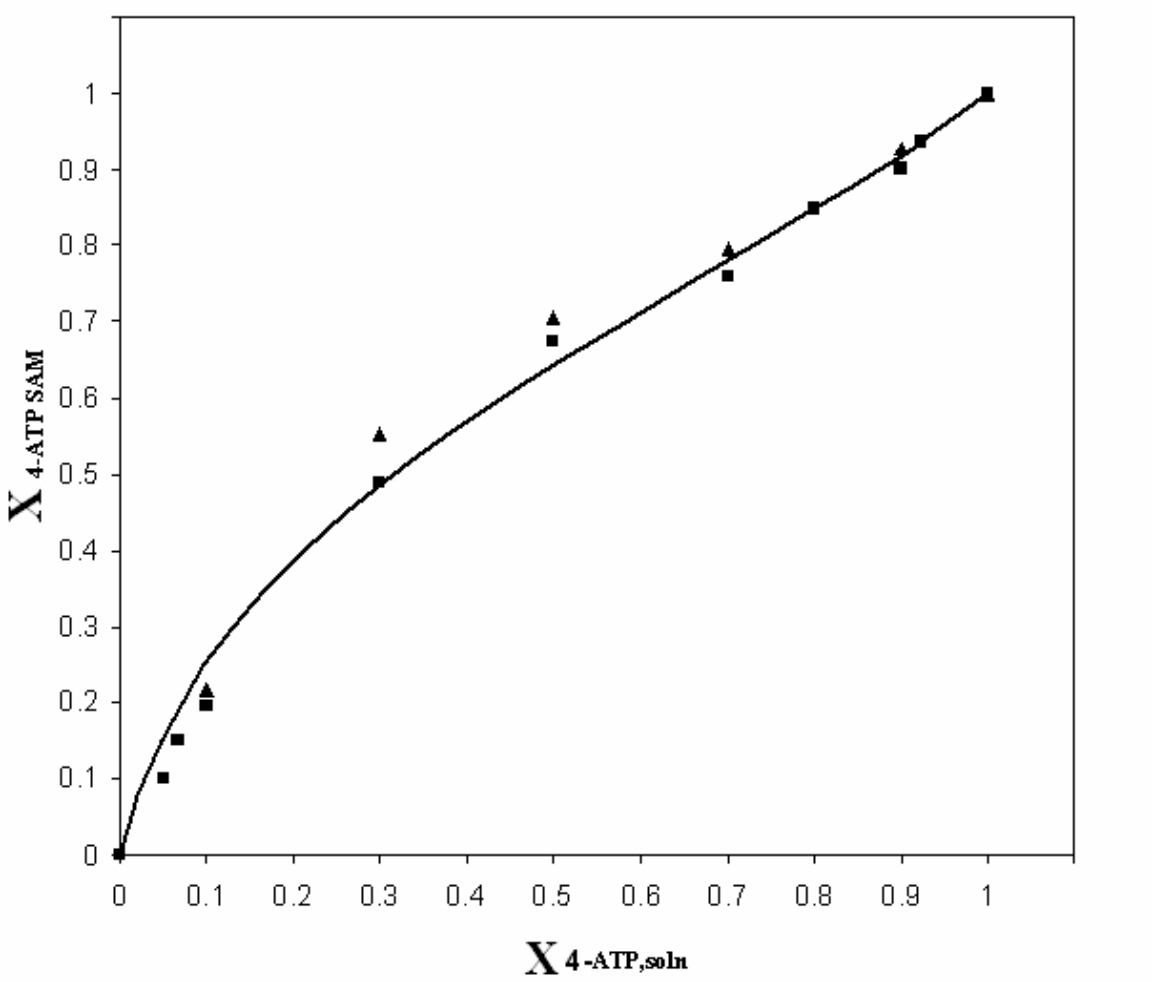

Fig. 2.11 Adsorption isotherms for 4-aminothiophenol/ EG_4-SH mixed monolayer. The mole fraction of 4-ATP on the monolayer surface determined by SERS and coulometry is plotted vs. the mole fraction of 4-ATP in the adsorption solution. (■) Isotherm determined using coulometry measurement. (▲) Isotherm determined using SERS.

.

2.3 References

1. Bain, C. D.; Whitesides, G. M. *J. Am. Chem. Soc.* **1988**, *110*, 6560.

2. Bain, C. D.; Whitesides, G. M. *Science (Washington, DC, United States)* **1988**, *240*, 62.

3. Bain, C. D.; Whitesides, G. M. *J. Am. Chem. Soc* **1988**, *110*, 3665.

4. Bain, C. D.; Evall, J.; Whitesides, G. M. *J. Am. Chem. Soc* **1989**, *111*, 7155.

5. Bain, C. D.; Whitesides, G. M. *J. Am. Chem. Soc* **1989**, *111*, 7164.

6. Chidsey, C. E. D.; Bertozzi, C. R.; Putvinski, T. M.; Mujsce, A. M. *J. Am. Chem. Soc* **1990**, *112*, 4301.

7. Evans, S. D.; Sharma, R.; Ulman, A. *Langmuir* **1991**, *7*, 156.

8. Rowe, G. K.; Creager, S. E. *Langmuir* **1991**, *7*, 2307.

9. Ulman, A.; Evans, S. D.; Shnidman, Y.; Sharma, R.; Eilers, J. E.; Chang, J. C. *J. Am. Chem. Soc* **1991**, *113*, 1499.

10. Laibinis, P. E.; Fox, M. A.; Folkers, J. P.; Whitesides, G. M. *Langmuir* **1991**, *7*, 3167.

11. Laibinis, P. E.; Whitesides, G. M. *J. Am. Chem. Soc* **1992**, *114*, 1990.

12. Folkers, J. P.; Laibinis, P. E.; Whitesides, G. M. *Langmuir* **1992**, *8*, 1330.

13. Laibinis, P. E.; Nuzzo, R. G.; Whitesides, G. M. *J. Phys. Chem.* **1992**, *96*, 5097.

14. Folkers, J. P.; Laibinis, P. E.; Whitesides, G. M.; Deutch, J. *J. Phys. Chem.* **1994**, *98*, 563.

15. Chailapakul, O.; Crooks, R. M. *Langmuir* **1993**, *9*, 884.

16. Imabayashi, S.-i.; Hobara, D.; Kakiuchi, T.; Knoll, W. *Langmuir* **1997**, *13*, 4502.

17. Hobara, D.; Ota, M.; Imabayashi, S.-i.; Niki, K.; Kakiuchi, T. *J. Electroanal. Chem.* **1998**, *444*, 113.

18. Hobara, D.; Sasaki, T.; Imabayashi, S.-i.; Kakiuchi, T. *Langmuir* **1999**, *15*, 5073.

19. Kakiuchi, T.; Sato, K.; Iida, M.; Hobara, D.; Imabayashi, S.-i.; Niki, K. *Langmuir* **2000**, *16*, 7238.

20. Kakiuchi, T.; Iida, M.; Gon, N.; Hobara, D.; Imabayashi, S.-i.; Niki, K. *Langmuir* **2001**, *17*, 1599.

21. Cooper, E.; Leggett, G. J. *Langmuir* **1999**, *15*, 1024.

22. Ong, T. H.; Waed, R. N.; Davies, P. B.; Bain, C. D. *J. Am. Chem. Soc.* **1992**, *114*, 6243.

23. Dimitrov, A. S.; Kralchevsky, P. A.; Nikolov, A. D.; Noshi, H.; Matusmoto, M. *J. Colloid Interf. Sci.* **1991**, *45*, 279.

24. Bain, C. D.; Troughton, E. B.; Tao, Y.-T.; Evall, J.; Whitesides, G. M.; Nuzzo, R. G. *J. Am. Chem. Soc.* **1989**, *111*.

25. Porter, M. D.; Bright, T. B.; Allara, D. L.; Chidsey, C. E. D. *J. Am. Chem. Soc***1987**, *109*, 3559.

26. Bain, C. D.; Whitesides, G. M. *J. Phys. Chem.* **1989**, *93*, 1670.

27. Laibinis, P. E.; Bain, C. D.; Whitesides, G. M. *J. Phys. Chem.* **1991**, *95*, 7017.

28. Offord, D. A.; John, C. M.; Linford, M. R.; Griffin, J. H. *Langmuir* **1994**, *10*, 883.

29. Stranick, S. J.; Parikh, A. N.; Tao, Y.-T.; Allara, D. L.; Weiss, P. S. *J. Phys. Chem.* **1994**, *98*, 7636.

30. Chidsey, C. E. D.; Loiacono, D. N.; Sleator, T.; Nakahara, S. *Surf. Sci.* **1988**, *200*, 45.

31. Collard, D. M.; Fox, M. A. *Langmuir* **1991**, *7*, 1192.

32. Hallmark, V. M.; Chaing, S.; Rabolt, J. F.; Swalen, J. D.; Wilson, R. *J. Phys. Rev. Lett.* **1987**, *59*, 2879.

33. Putnam, A.; Blackford, B. L.; Jericho, M. H.; Watanbe, M. O. *Surf. Sci.* **1989**, *217*, 276.

34. Vance, J.; Reiss, G.; Schneider, F.; Bauer, K.; Hoffmann, H. *Surf. Sci.* **1989**, *218*, 108.

35. Creager, S. E.; Hochett, L. A.; Rowe, G. K. *Langmuir* **1992**, *8*, 854.

36. Chailapakul, O.; Crooks, R. M. *Langmuir* **1995**, *11*, 1329.

37. Bragg, W. L.; Williams, E. *J. Rroc. R. Soc. London* **1936**, *145*, 699.

38. Jaroniec, M. P. *J. Colloid Polymn. Sci.* **1980**, *258*, 977.

39. Xing, X. F.; Li, S. F. Y.; Lau, A. K. H.; O'Shes, S. J. *J. electroanal. Chem.* **2005**, *583*, 124.

40. Li, F. P. *Master's Thesis, Auburn Univ., Auburn, AL, USA.,* **2004**.

41. Widrig, C. A.; Chung, C.; Porter, M. D. *J. Electroanal. Chem. Interf. Electrochem.* **1991**, *310*, 335.

42. Hayes, W. A.; Shannon, C. *Langmuir* **1996**, *12*, 3688.

43. Yue, X. H. *Electrochemical studies of mixed monolayers on gold surfaces and an AFM investigation of thrombin catalyzed fibrin formation on PVC membranes; M.S. Thesis* **1999**, *Auburn University, Auburn*, AL.

44. Vanderah, D. J.; Valincius, G.; Meuse, C. W. *Langmuir* **2002**, *18*, 4674.

45. Vanderah, D. J.; Arsenault, J.; La, H.; Gates, R. S.; Silin, V.; Meuse, C. W. *Langmuir* **2003**, *19*, 3752.

46. Vanderah, D. J.; Parr, T.; Silin, V.; Meuse, C. W.; Gates, R. S.; La, H. *Langmuir* **2004**, *20*, 1311.

CHAPTER 3

QUANTIFICATION OF NONSPECIFIC ADSORPTION ON MIXED SAM BIOSENSOR PLATFORMS USING ELECTROCHEMICAL ENZYME IMMUNOASSAY

3.1 Quantification of protein adsorption on mixed SAMs of decanethiol and tetraethylene glycol thiol using electrochemical enzyme immunoassay

3.1.1 Introduction

With the development of immunoassays, more and more immunochemical techniques have been used in the application of biosensors. In order to increase the sensitivity and selectivity of the biosensors, many techniques such as sandwich assay, enzyme assay and competitive assay [1-3] have been developed to generate and enhance the signals of biomolecular interactions, for example antigen-antibody complexation[4], and DNA hybridization. Enzyme immunoassay (EIA) is an assay that uses an enzyme-bound antibody to detect antigens[5]. The enzyme catalyzes a reaction when exposed to a substrate. This study uses an enzyme immunoassay coupled with electrochemical detection. Electrochemical enzyme immunoassay is based on the conversion of an electroinactive substrate to an electroactive product by the enzyme and has been developed to analyze antibodies and antigens under enzyme catalysis[6-8]. The enzyme should fulfill several requirements: it must produce electrochemically active products; it

must have a high K_{cat} (catalysis efficiency); the enzyme and enzyme substrates must be stable in buffer solution; and there must be few by-product of the enzyme reaction.

For the assay processes, anti-rabbit IgG (antibody) labeled with the enzyme-alkaline phosphatase (AP) was used for protein adsorption and directly physically adsorbed onto the mixed SAM monolayer containing decanethiol (DT) and tetraethylene glycol thiol (EG_4-SH) in varying molar ratios. Due to the high turnover number and broad substrate specificity, alkaline phosphatase is one of the most important enzymes. It can convert *p*-aminophenyl phosphate (*p*APP) to *p*-aminophenol (*p*AP) (Scheme 3.1.a.), which is a strongly electroactive compound in buffer solution and can be oxidized to *p*-aminophenoxyl (Scheme 3.1.b)[9,10]. After the enzyme reaction and electrochemical reaction have occurred, the current of the oxidative peak can be recorded using cyclic voltammetry. Because of the low redox potential of its hydrolysis product *p*-aminophenol, the large difference in redox potential between its de- and phosphorylated forms, and the absence of electrode fouling by electropolymerization[11], *p*-aminophenyl phosphate is generally considered to be the most suitable substrate for alkaline phosphatase. Several studies have shown that alkaline phosphatase has the best catalytic activity at pH 9.0, and the base line signal of control experiment caused by *p*APP non-enzymatic hydrolysis is the smallest in Tris buffer solution. Thus, the amount of *p*-aminophenol in buffer solution can be determined based on the current density of the oxidative peak. The amount of protein adsorption (labeled antibody) onto the mixed monolayer is proportional to the amount of *p*-aminophenol, so the protein adsorption on the mixed SAM monolayer with various molar ratios of DT and EG_4-SH can be quantified.

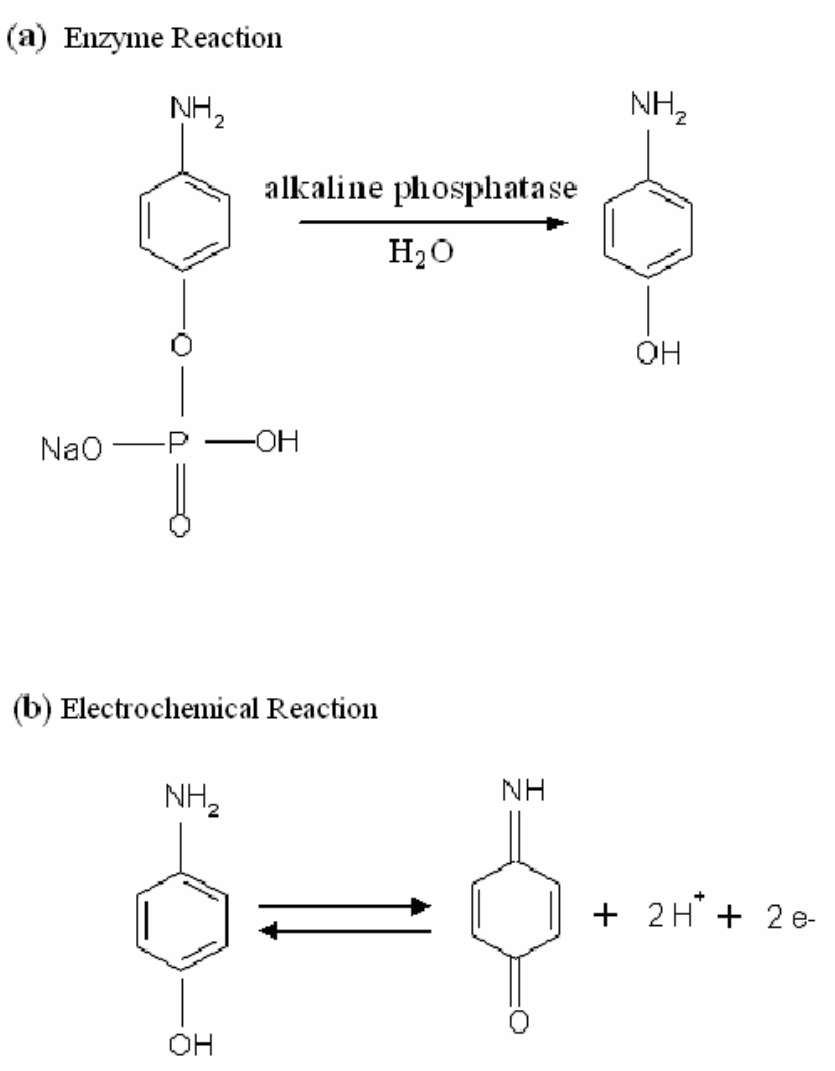

Scheme 3.1 Schematic representation of (a) enzyme reaction in which alkaline phosphatase catalyzes the conversion of *p*-aminophenyl phosphate (*p*APP) to *p*-aminophenol (*p*AP), and (b) electrochemical reaction between *p*-aminophenol and *p*-aminophenoxyl

3.1.2 Experimental

Chemicals and materials Sodium chloride, magnesium chloride, sodium phosphate (dibasic anhydrous), sodium phosphate (monobasic), sulfuric acid, hydrochloric acid and sodium hydroxide were bought from Fisher. Tris(hydroxymethyl)aminomethane and Tween-20 were bought from ACROS. Sodium perchlorate, 4-nitrophenylphosphate disodium salt (99 %) and sodium sulfide were bought from Alfa Aesar. Alkaline phosphatase conjugated monoclonal anti-rabbit IgG (γ-chain-specific) was obtained from Sigma Chemical Co. and used as received.

Reagent synthesis 4-Aminophenylphosphate (*p*APP) was synthesized by reduction of 4-nitrophenyl phosphate. Briefly, 2.3 g of 4-nitrophenyl phosphate disodium salt (Na_2 – *p*NPP) was dissolved in 5.6 mL of distilled water and the pH adjusted to 9 with NaOH solution. Then 3.0g $Na_2S{\cdot}9H_2O$ was added and the mixture was heated to 90 – 95 °C for 1 hour. The solution was cooled and acidified with concentrated HCl (pH < 2). The acidified solution was filtered and the pH was adjusted to 4-5 by NaOH solution. The white crystals (the monosodium salt of *p*APP) were collected and recrystallized from methanol to remove inorganic impurities. The product *p*APP was refrigerated for later use.

Buffer solutions The buffer solutions used in the experiment were as follows: Buffer A: 0.135 M NaCl + 1% (v/v) Tween-20; Buffer B: 0.1 M Tris (hydroxymethyl) aminomethane, 1 mM magnesium chloride, and 0.02% (w/v) sodium azide. The pH was adjusted to 9.0 with concentrated hydrochloric acid solution.

Solutions 5 μg/mL anti-rabbit IgG alkaline phosphatase conjugate solution was prepared by diluting from stock solutions separately with buffer A. The substrate solution

was 4 mM 4-aminophenyl phosphate in buffer B and was prepared before use in order to minimize the non-enzymatic hydrolysis of *p*APP in the solution.

Covalent immobilization of immunoreagents Au foil (99.999% purity, Alfa) was cleaned by soaking sequentially in distilled water, piranha solution (1: 3 H_2O_2:H_2SO_4), and distilled water. The mixed SAM monolayers were prepared by immediately immersing the gold electrode in 1.0×10^{-3} mol/L solutions of the corresponding thiol in 95% ethanol for 24 hr. Upon removal from the thiol solution, the SAMs were rinsed with ethanol and dried with nitrogen. The gold electrode modified with mixed SAM monolayer was soaked in 5 μg/mL anti-rabbit IgG alkaline phosphatase conjugate solution for half an hour at room temperature. After being taken out of the labeled antibody solution, the electrode was rinsed by distilled water then transferred into a Teflon electrochemical cell containing 4 mM 4-aminophenyl phosphate in 0.1 M Tris buffer (pH 9.0) solution. The alkaline phosphatase label catalyzes the conversion of 4-aminophenyl phosphate to 4-aminophenol, which can be easily detected by cyclic voltammetry. Oxidative peak currents were recorded.

Electrochemistry All cyclic voltammetry experiments were performed in a homemade Teflon cell with a total volume of 10 mL. A standard three-electrode system was used in which a gold foil was the working electrode, a Pt wire was the counter electrode and Ag/AgCl was the reference electrode. All potentials were referenced to the reference electrode. The scanning rate was 100mV/s. The electrochemical cell was isolated from light with aluminum foil and maintained in a nitrogen atmosphere during the immunoassay experiments.

3.1.3 Results and discussion

Mixed self-assembled monolayers of DT and EG_4-SH in various molar ratios were used and anti-rabbit IgG labeled with alkaline phosphates physically directly adsorbed onto the mixed SAM monolayer. Such adsorption is nonspecific adsorption. The label used was alkaline phosphatase, which catalyzes *p*-aminophenyl phosphate (*p*APP) to *p*-aminophenol (*p*AP), an electroactive compound. This product can be detected by electrochemistry and thus generate the CV signal. By measuring the current density of the redox peak, the amount of *p*-aminophenol could thus be determined. Finally, the amount of protein adsorption (labeled anti-rabbit IgG) on the mixed monolayer with various mole fractions of EG_4-SH in mixed SAM monolayers of EG_4-SH /Decanethiol was determined.

The cyclic voltammetric response of *p*-aminophenol for labeled anti-rabbit IgG physically adsorbed onto gold surfaces respectively modified with EG_4-SH and DT-SAM monolayers in 4 mM 4-aminophenyl phosphate and 0.1 M Tris buffer (pH 9.0) solutions is shown in Fig. 3.1. The baseline curve comes from a blank experiment. By subtracting the baseline current density from the current density of *p*-aminophenol for the labeled antibody on pure DT-SAM, the amount of protein adsorption on the DT-SAM surface can be determined. The same method was used to obtain the amount of protein adsorption on a pure EG_4-SH monolayer surface. The figure clearly shows that protein adsorption on DT-SAM is much higher than on the EG_4-SH SAM surface. A series of cyclic voltammetric data of *p*-aminophenol for labeled anti-rabbit IgG adsorptions on gold surfaces with mixed SAM monolayers formed by adsorption from solutions containing EG_4-SH and alkanethiol in varying molar ratios plotted as a function of mole fraction of EG_4-SH in the SAM monolayer are shown in Fig. 3.2. As the mole fraction of EG_4-SH

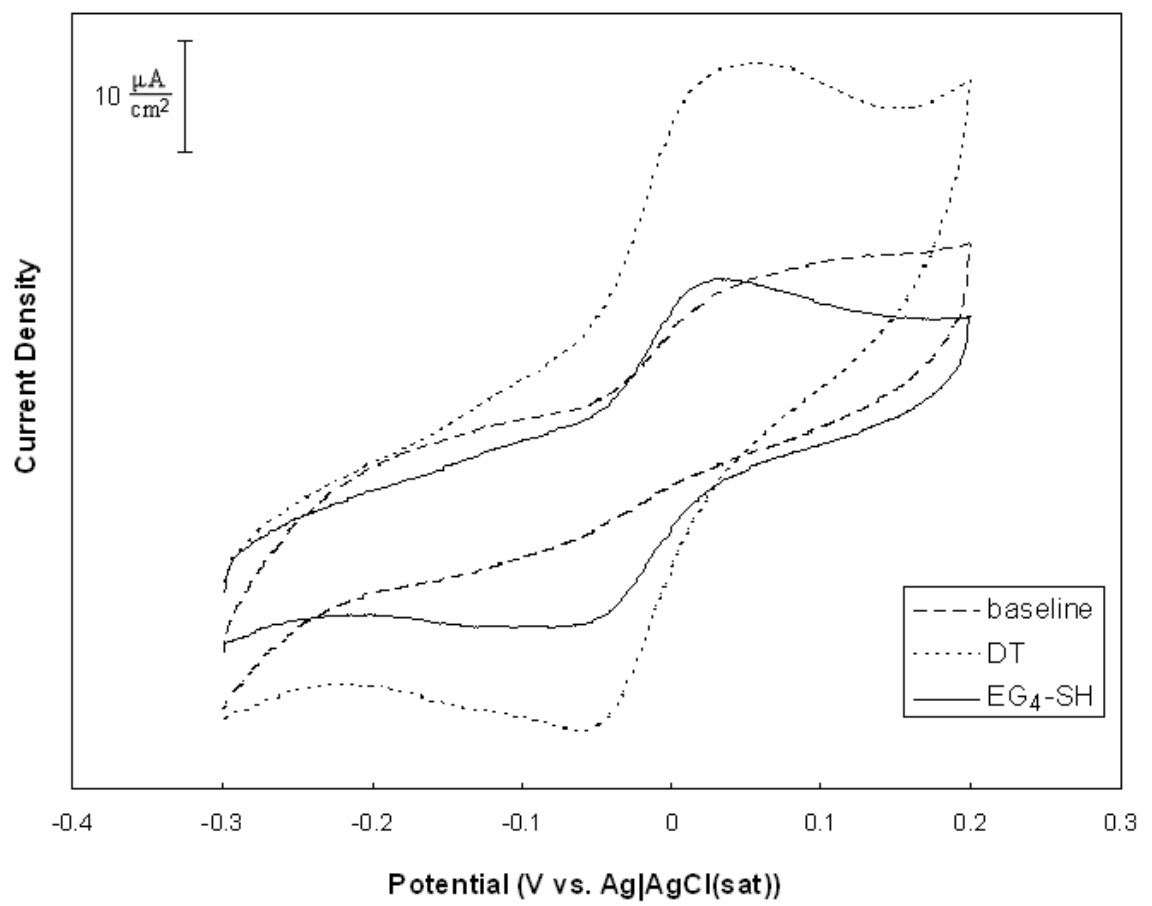

Fig. 3.1. Typical cyclic voltammograms of *p*-aminophenol for labeled anti-rabbit IgG physically adsorbed on gold electrodes individually modified with EG_4-SH and DT-SAM monolayers in a solution containing 4 mM 4-aminophenyl phosphate and 0.1 M Tris buffer (pH 9.0).

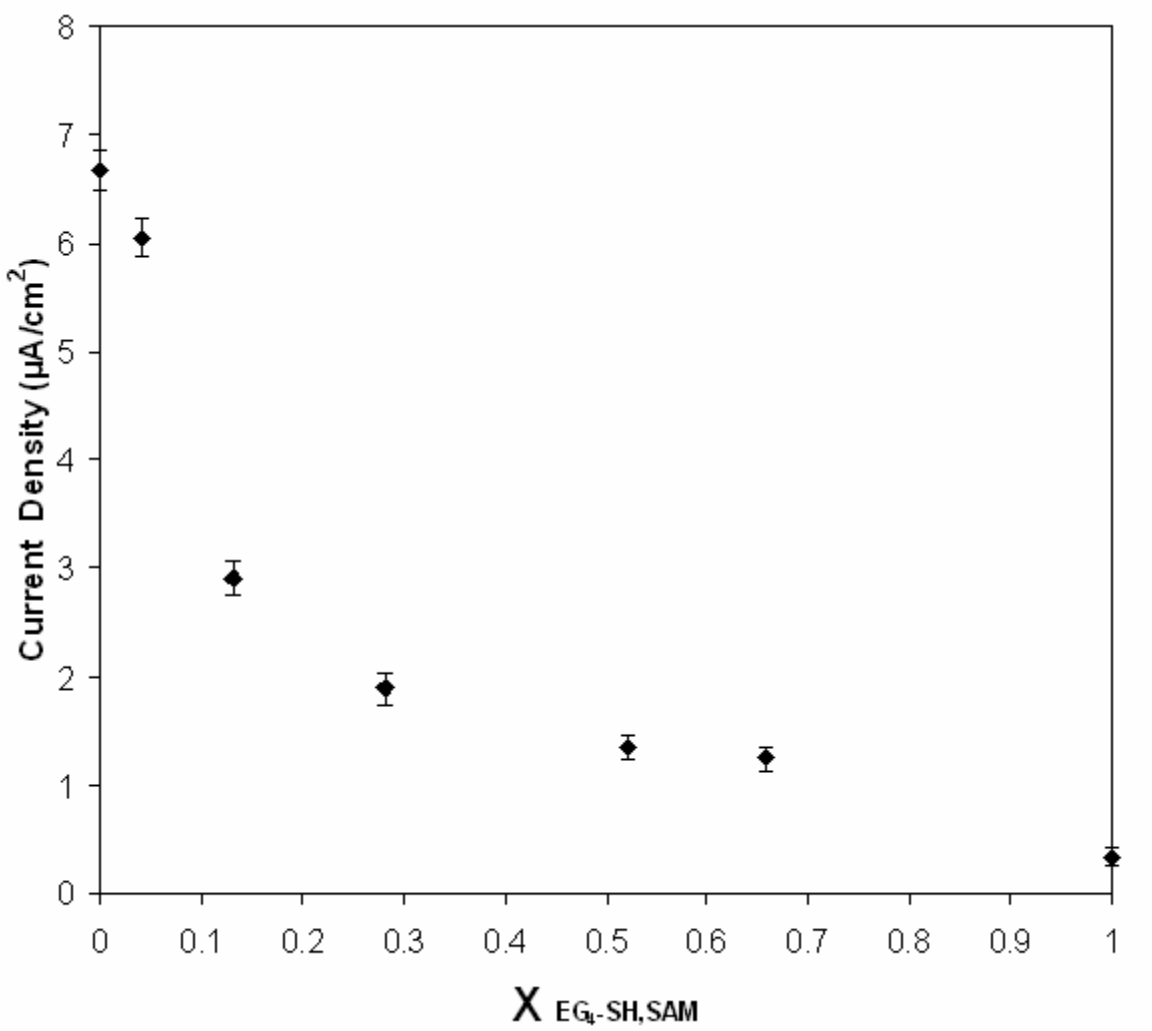

Fig.3.2. Plot of oxidative current density of *p*-aminophenol for labeled antibodies physically adsorbed on EG_4-SH/DT mixed monolayers as a function of the mole fraction of EG_4-SH in the SAM.

increases, the protein adsorption on the SAM surface with the corresponding mole ratios of EG_4-SH and alkanethiol decrease. Comparing two data points, namely $\chi_{EG4\text{-}SH,\ SAM} = 0$ and $\chi_{EG4\text{-}SH,\ SAM} = 1$, reveals that labeled anti-rabbit IgG adsorption on pure EG_4-SH SAMs decreases by a more than twenty fold compared to that adsorbed on a pure DT-SAM surface. This indicates that proteins are strongly adsorbed on hydrophobic DT-SAM but not strongly adsorb on hydrophilic EG_4-SH SAM. The EG_4-SH monolayer thus offers a better non-fouling surface than DT-SAM. This figure also shows that when the mole fraction of EG_4-SH in the SAM monolayer is below 0.2, the current density decreases quickly. Above 0.2, however, the rate of decrease becomes slower, suggesting that when the mole fraction of EG_4-SH in the SAM is more than 0.2, DT-SAM but not strongly adsorb on mixed monolayer has adequate resistance to protein adsorption.

3.2 Application of DT or EG_4-SH SAM resistance to nonspecific adsorption on electrochemical immuno-sandwich mixed SAM biosensor platforms

3.2.1 Introduction

To further compare the resistance of alkanethiol and tetraethylene glycol thiol to protein adsorption, nonspecific adsorption on electrochemical immuno-sandwich sensor platforms with mixed SAM monolayers were studied using alkanethiol and tetraethylene glycol thiol as blocking agents. In a typical electrochemical immuno-sandwich assay (shown in scheme 3.2), a gold substrate was first modified with a mixed SAM monolayer of 4-ATP and a blocking agent, such as an alkanethiol, and oligo(ethylene glycol). Polyaniline (PANI) film was then electrochemically deposited on the mixed monolayer by nucleophilic reaction between polyaniline and amino group of 4-ATP molecule,

providing a semiconducting membrane to attach the unlabeled antibody (anti-rabbit IgG) onto the sensor surface. After the unlabeled antibody was immobilized on surface, the biosensor surface was able to capture the target antigen (rabbit IgG) from a biological sample through a specific biomolecular interaction between the unlabeled antibody and target antigen. The labeled antibody (anti-rabbit IgG conjugated with alkaline phosphatase) was then combined with the target antigen rabbit IgG and immobilized on the electrode surface. By same enzyme reaction as that involved in converting of *p*-aminophenyl phosphate (*p*APP) to *p*-aminophenol (*p*AP) and the electrochemical processes of redox of *p*-aminophenol, reported in section 3.1.2, a redox current peak of cyclic voltammogram is obtained. From the current density of the redox peak, the amount of labeled antibody could then be determined. Finally the amount or concentration of target antigen in biological sample was found based on the specific interaction between the target antigen and labeled antibody.

Due to its high electrical conductivity, ease of use and durability, polyaniline was chosen for use as the conjugated polymer[12-15]. In acidic and PH-neutral solutions, charged PANI, which has electrical conductivity and electrochemical activity, facilitates the direct and mediated electron exchange between the active centers of biomolecules and polymer films. Polyaniline has three forms, namely the emeraldine form, the leucoemaraldine form and the pernigraniline form. By sweeping a potential, these forms can be converted to each other. Emeraldine form is the most stable and useful form for conjugating antibodies and 4-aminothiophenol[16]. Polyaniline can be synthesized by several methods, such as the chemical oxidization of aniline monomer[17-21] and the electrochemical

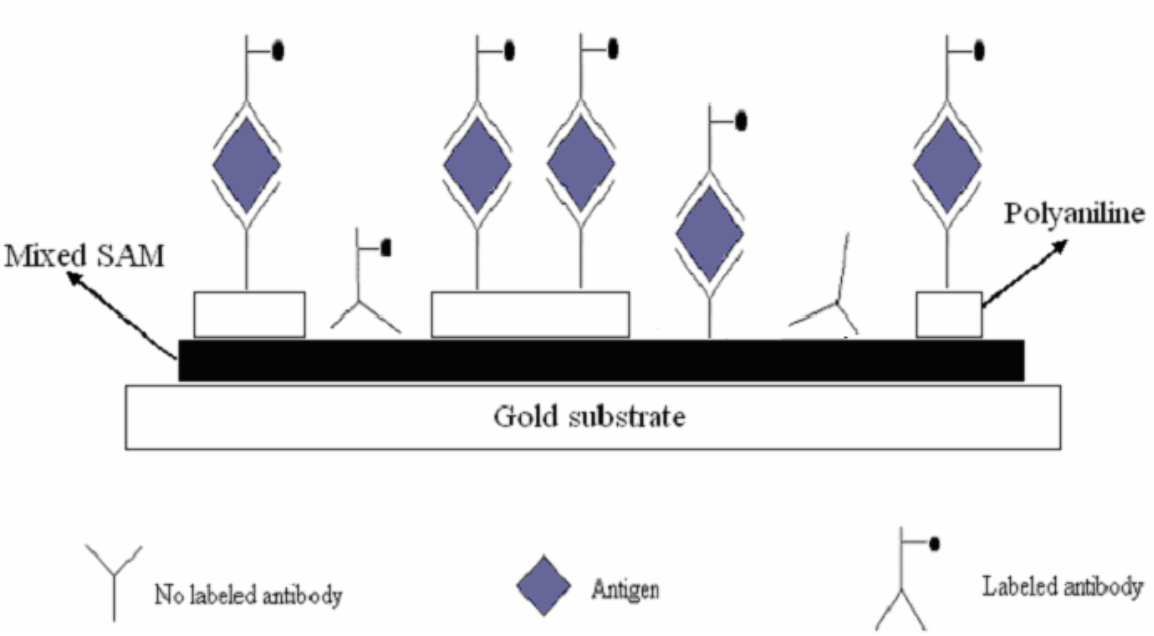

Scheme 3.2 Schematic presentation of electrochemical immuno-sandwich assay.

polymerization of aniline[22-24]. Here controlled potential electrolysis was used, applying a constant potential to a working electrode to polymerize the aniline and form an oxidized PANI film (emeraldline form). PANI film can react with a number of nucleophiles, such as amine or thiol groups on the molecules. IgG protein molecule includes nucleophilic groups and can be immobilized on the surface by the covalent interaction between polyaniline and the nucleophilic groups in antibodies.

The objective here was to apply an electrochemical immuno-sandwich biosensor to compare the resistance to nonspecific adsorption, so an antigen solution with a fixed concentration was used throughout. The amount of the labeled antibody calculated from the current density of the oxidative peak contains specific adsorption caused by proteins chemically adsorbed onto the mixed SAM modified with polyaniline thin film, and nonspecific adsorption caused by the antigen or antibody physically adsorbed onto the mixed SAM surface. If the amounts of specific adsorption chemically adsorbed on DT/ATP and EG_4-SH/ATP monolayer surface modified with PANI are the same, nonspecific adsorption adsorbed on these two mixed SAM surfaces can be compared by examining the magnitude of the oxidative current densities.

3.2.2 Experimental

Chemicals and materials Aniline monomer (Fisher) was distilled under reduced pressure over zinc metal prior to use and stored in the dark at 4 °C in a nitrogen gas atmosphere. All other chemicals were reagent grade and used as received. Affinipure anti-rabbit IgG, rabbit IgG, alkaline phosphatase conjugated monoclonal anti-rabbit IgG (γ-chain-specific) were obtained from Sigma Chemical Co. and used as received.

Solutions 5 μg/mL anti-rabbit IgG solution (unlabeled antibody), rabbit IgG solution (antigen) and anti-rabbit IgG alkaline phosphatase conjugate solution (labeled antibody) were prepared by diluting from stock solutions separately with 0.135 M NaCl + 1% (v/v) Tween-20. The support electrolyte for cyclic voltammetry was 4 mM 4-aminophenyl phosphate in Tris (hydroxymethyl) aminomethane (pH 9) buffer.

Electropolymerization of aniline on mixed SAM surfaces and covalent immobilization of immunoreagents After the Au electrode was immersed in a mixed thiol solution containing 4-ATP and DT or 4-ATP and EG4-SH for 24 hr, a polyaniline film was electrodeposited on the gold foil electrode using 0.05 M aniline monomer in 0.5 M H_2SO_4 aqueous solution. The electropolymerization of aniline was carried out by controlled potential electrolysis at 800 mV (*vs.* Ag/AgCl) for 3 minutes. The oxidized form was prepared by applying 600 mV on the polyaniline electrode for 3 minutes in 0.5 M sulfuric acid solution. The polyaniline-coated electrodes were cleaned by soaking in deionized water three times for 3 minutes each to remove aniline and acid residue.

In the sandwich immunoassay, an electrode with the polyaniline film was firstl soaked in 5 μg/mL anti-Rabbit IgG solution for 1 hour at room temperature and then rinsed in a buffer solution of 0.135 M NaCl + 1% (v/v) Tween-20. Secondly the modified electrode was soaked in 5 μg/mL antibody solution, and then in 5 μg/mL alkaline phosphatase labeled antibody for half an hour each. After being removed from the labeled antibody solution, the electrode was rinsed with distilled water. Finally the substrate was transferred into a Teflon electrochemical cell containing 4 mM 4-aminophenyl phosphate in 0.1 M Tris buffer (pH 9.0) solution. The alkaline phosphatase label catalyzed the

conversion of 4-aminophenyl phosphate to 4-aminophenol, which can be easily detected by cyclic voltammetry. Oxidative peak currents were then recorded.

3.2.3 Results and discussion

An electrochemical immuno-sandwich assay was used to confirm that nonspecific adsorption on a mixed SAM monolayer modified with 4-ATP and EG_4-SH is reduced compared with nonspecific adsorption on the mixed SAM monolayer modified with 4-ATP and DT. A 4-ATP SAM monolayer was used to immobilize a polyaniline film on the biosensor surface by covalent bonds between the polyaniline and the amino groups on the 4-ATP biomolecules. Unlabeled antibody was immobilized on the monolayer surface through the polyaniline film. After a fixed concentration of antigen was combined with the unlabeled antibody, labeled antibodies were attached to the biosensor surface by specific biomolecular interaction between the antigen and antibody, providing a CV signal. This electrochemical signal indicates the specific adsorption caused by the protein chemically adsorbed on the polyaniline thin film, and also the nonspecific adsorption caused by protein physical adsorption.

Before discussing the nonspecific adsorption on immuno-sandwich sensors, the specific adsorption must first be studied. The specific adsorption is proportional to the amount of polyaniline deposited on the mixed SAM monolayer. The voltammetric behavior of polyamine thin film on 4-ATP/ EG_4-SH mixed monolayers with a mole fraction of 4-ATP of 0.48 immersed in 0.10M $HClO_4$ supporting electrolyte is shown in Fig. 3.3. In this experiment, the scan was initiated at a potential of 0.0 V, swept positive to an upper limit of 1.0 V, and then swept cathodically back to 0.0 V at a scan rate of 100 mV/s. The

wave (A1) at 0.15V corresponds to the oxidation of leucoemaraldine form of the polyanline to emeraldine, and the wave centered at 0.73V corresponds to the further oxidation of the emeraldine form of PANI to the pernigraniline form. The peak positions did not shift as a function of the mole fraction of EG_4-SH in the SAM. Both peaks are useful to determine the amount of polyamine film on mixed SAMs with different mole fractions of EG_4-SH in the SAMs. Here, the charge under peak A2 is used to measure the amount of polyaniline film on the mixed SAM. Several PANI films grown on 4-ATP/DT or 4-ATP/EG_4-SH SAM-modified Au electrodes with various mole fractions of 4-ATP in the SAM were used to study the influence of different two-component mixed monolayer systems on the electrodeposition of polyaniline thin films. The cyclic voltammetric data under peak A2 of polyaniline for the different two-component mixed SAM surfaces with various mole fractions of 4-ATP in the SAM are presented in Table 3.1.

Table 3.1 Current density (A) of polyaniline on different mixed SAM

$X_{4\text{-ATP, SAM}}$	4-ATP/EG_4-SH	4-ATP/DT
0.15	0.42×10^{-4}	0.47×10^{-4}
0.48	1.15×10^{-4}	1.13×10^{-4}
0.78	2.37×10^{-4}	2.50×10^{-4}

For these two SAMs, 4-ATP/EG_4-SH and 4-ATP/DT, when the mole fraction of 4-ATP in the monolayer were the same, the current densities of polyaniline on these two mixed SAM systems were similar. Because the specific adsorption is proportional to the amount of polyaniline on SAM surface, for the same mole fraction of 4-ATP in the SAM, the specific adsorption on the 4-ATP/EG4-SH mixed monolayer will be the same as that

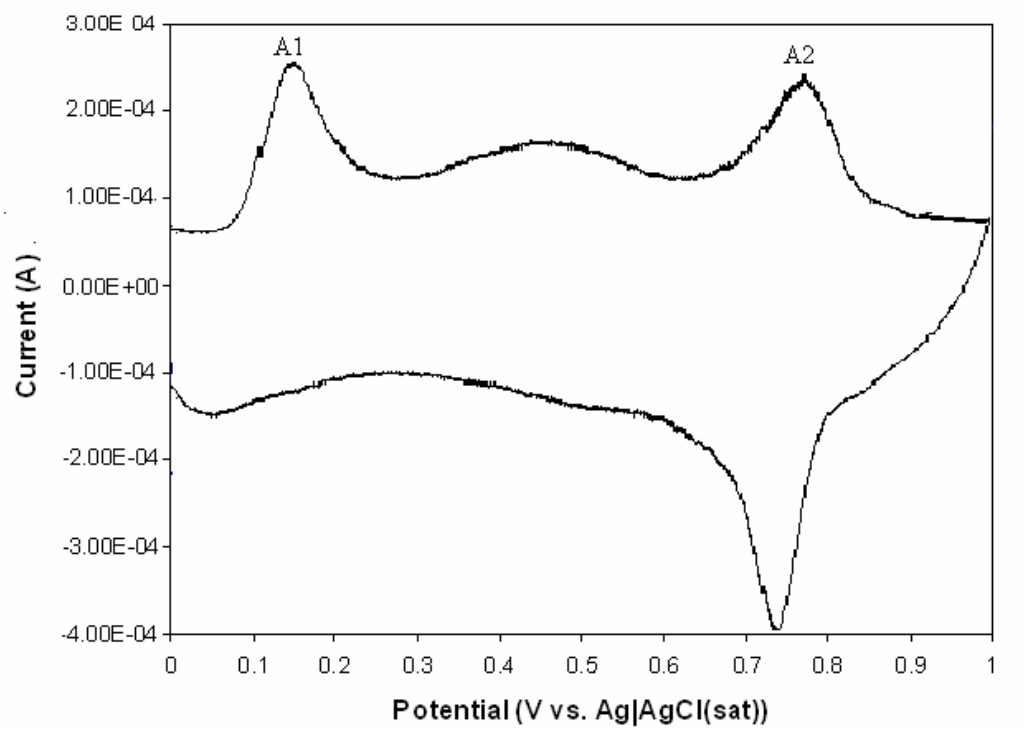

Fig. 3.3 Voltammetric signatures of polyaniline thin films grown on 4-ATP/ EG_4-SH mixed monolayers with a mole fraction of 4-ATP of 0.48

on 4-ATP/DT mixed SAM monolayer, so the nonspecific adsorption on both mixed SAM surface can be individually compared. By using an electrochemical immuno-sandwich assay, a series of cyclic voltammograms of *p*-aminophenol were achieved similar to those shown in Fig. 3.1. The oxidative current density of *p*-aminophenol for protein adsorption on an electrochemical immuno-sandwich sensor surface modified with a two-component mixed monolayer of 4-ATP and a blocking agent (DT or EG_4-SH) as a function of the mole fraction of a blocking agent in the mixed SAM monolayer is presented in Fig. 3.4. For both mixed SAM systems, the current densities decreased as the mole fraction of the blocking agent in the SAM increased. At a specific mole fraction of blocking agent in the SAM, for example at 0.52, the protein adsorption on 4-ATP/EG_4-SH mixed SAM was lower than the protein adsorption on 4-ATP/DT SAM surface. By comparing the last two data points, which correspond to $\chi = 1$ (pure blocking agent without 4-ATP), the nonspecific adsorption on pure EG_4-SH SAM is reduced more than fifteen fold compared to its value on a pure DT-SAM surface. This result confirms that EG_4-SH is a better blocking agent for the inhibition of protein adsorption than decanethiol, and EG_4-SH can be used to replace DT to manufacture an immuno-sandwich sensor with mixed SAM monolayers.

To gain a better understanding of how EG_4-SH resistance to nonspecific adsorption compares to that of DT, the data in Fig. 3.4 is replotted in Fig. 3.5, which shows the ratio of current densities for the two mixed SAM systems as a function of 4-ATP in the SAM. A sharp break occurs at a mole fraction of 4-ATP in the SAM of around 0.15. This indicates that when the mole fraction of 4-ATP in the mixed SAM is less than 0.15, EG_4-SH/4-ATP monolayer is good enough to reduce nonspecific adsorption. Earlier in

the chapter, the EG_4-SH/DT mixed SAM resistance to nonspecific adsorption by immunoassay was examined, which included only the labeled antibody. That result showed that when the mole fraction of EG_4-SH exceeded 0.2, the EG_4-SH/DT SAM surface is good enough to reduce nonspecific adsorption. In the immuno-sandwich assay, however, the mole fraction of EG_4-SH in the SAM must be more than 0.85, and EG_4-SH/ATP-SAM has a better resistance to nonspecific adsorption than DT/ATP-SAM. This indicates that EG_4-SH does not increase its resistance to nonspecific adsorption much more than DT. The reason is that in real biosensor devices, the electrochemical signal due to specific adsorption is much bigger than the signal due to nonspecific adsorption.

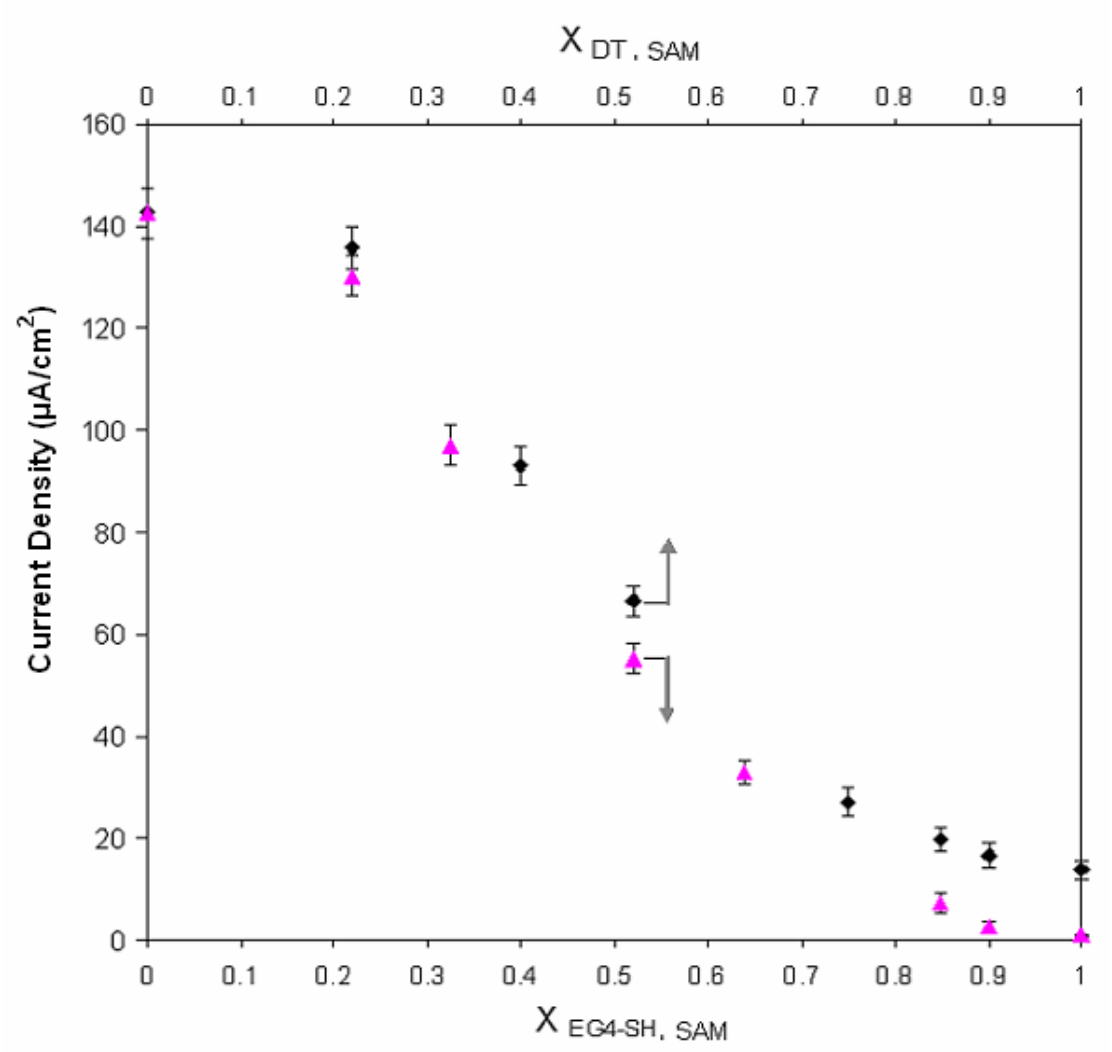

Fig. 3.4 Plot of current density vs. mole fraction of DT in 4-ATP/DTmixed SAM monolayers (♦) and plot of current density vs. mole fraction of EG_4-SH in 4-ATP/EG_4-SH mixed SAM monolayers (▲). The current density is caused by protein adsorption on mixed SAM surface, which includes specific adsorption and nonspecific adsorption.

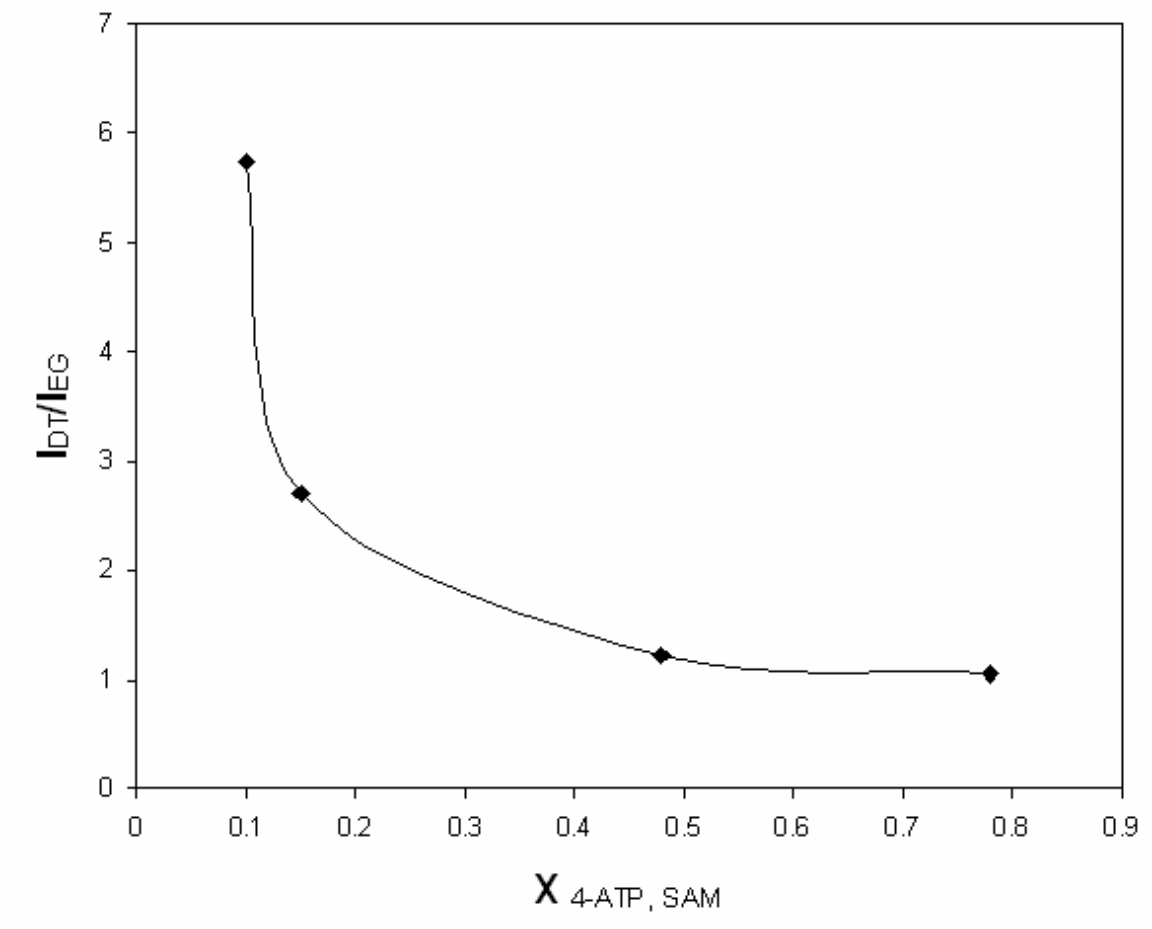

Fig.3.5. Ratio of current densities of *p*-aminophenol for protein adsorption on 4-ATP/DT-SAM and 4-ATP/EG_4-SH SAM surfaces as a function of the mole fraction of 4-ATP in the SAM

3.3 References

1. Medyantseva, E. P.; Khaldeeva, E. V.; Budnikov, G. K. *J. Anal. Chem.* **2001**, *56*, 886.

2. Song, W. C. *Curr. Dir. Autoimmun.* **2004**, *7*, 181.

3. Warsinke, A.; Benkert, A.; Scheller, F. W. *J. Anal. Chem.* **2000**, *366*, 622.

4. Sadana, A.; Beelaram, A. M. *Biosens. Bioelectron.* **1995**, *10*, 301.

5. Maertlbauer, E. *Food Authenticity and Traceability* **2003**, 54.

6. Wehmeyer, K. R.; Halsall, H. B.; Heineman, W. R. *Anal. Chem* **1986**, *58*, 135.

7. Dong, Y. Z.; Shannon, C. *Anal. Chem.* **2000**, *72*, 2371.

8. Aguilar, Z. P.; Vandaveer, W. R.; Fritsch, I. *Anal. Chem.* **2002**, *74*, 3321.

9. Nebling, E.; Grunwald, T.; Albers, J.; Schafer, P.; Hintsche, R. *Anal. Chem.* **2004**, *76*, 689.

10. Kim, E.; Kim, K.; Yang, H.; Kim, Y. T.; Kwak, J. *Anal. Chem.* **2003**, *75*, 5665.

11. Treloar, P. H. N., A. T.; Kane, J. W. *Electroanal.* **1994**, *6*, 561.

12. Moore, E. J.; Pravda, M.; Kreuzer, M. P.; Guilbault, G. G. *Anal. Lett.* **2003**, *36*, 303.

13. Pron, A.; Rannou, P. *Prog. Polym. Sci.* **2002**, *27*, 135.

14. Nicolas, D. D.; Poncin, E. F. *Anal. Chim. Acta* **2003**, *475*, 1.

15. Malinauskas, A. *J. Power Sources* **2004**, *126*, 214.

16. Li, F. P. *Electrochemical studies of underpotential deposition with surface plasmon resonance and enzyme immunoassay; M.S. Thesis, 2004, Auburn University, Auburn, AL*.

17. Hatchett, D. W.; Kinyanjui, J. M.; Smith, A.; Josowicz, M. *Polym.* **2004**, *45*, 143.

18. Campos, T. L. A.; Kersting, D. F.; Ferreira, C. A. *Surf. Coat. Tech.* **1999**, *122*, 3.

19. Kulkarni, M. V.; Viswanath, A. K. *Eur. Polym. J.* **2004**, *40*, 379.

20. Anitha, G.; Subramanian, E. *Sens. and Actuators B* **2003**, *B92*, 49.

21. Athawale, A. A.; Kulkarni, M. V.; Chabukswar, V. V. *Mater. Chem. and Phys.* **2002**, *73*, 106.

22. Mohilner, D. M.; Adams, R. N.; Argersinger, W. J. *J. Am. Chem. Soc.* **1962**, *84*, 3618.

23. Zhou, H. H.; Jiao, S. Q.; Chen, J. H.; Wei, W. Z.; Kuang, Y. F. *Thin Solid Films* **2004**, *450*, 233.

24. Boehme, J. L.; Mudigonda, D. S. K.; Ferraris, J. P. *Chem. Mater.* **2001**, *13*, 4469.

CHAPTER 4

CONCLUSIONS

4.1 Characterization of two-component organothiol mixed monolayers on gold.

Mixed SAMs containing EG_4-SH/alkanethiol with different chain lengths were characterized by capacitance measurement and discussed in terms of the model of thermodynamic control in the formation of mixed monolayer. The results indicate that for alkanethiols with different chain lengths, the longer the chain length, the smaller the $\Delta\mu$, and the stronger the adsorption tendency on gold. For these three mixed SAM systems, ω are all less than zero, which means that interactions between EG_4-SH and alkanethiol are more energetically favorable than interactions between EG_4-SH and EG_4-SH or alkanethiol and alkanethiol. ω becomes more negative as the chain length of alkanethiol increases, which indicates that the interactions between EG_4-SH and alkanethiol become stronger. In these SAM systems, EG_4-SH is similar with shorter chain alkanethiols, which have a richer solvation in ethanol and a weaker tendency to come out of the solution and adsorb onto the gold surface.

Two-component mixed monolayers of 4-ATP/DT were studied by coulometry measurements. Based on the results, decanethiol molecules, which have a poorer solvation in ethanol and a stronger tendency to form a well-ordered two-dimensional

crystalline film on the gold in the absence of a coadsorbate, become disordered in the presence of the much shorter 4-ATP.

Mixed EG_4-SH/4-ATP SAM systems were characterized by SERS and coulometry measurement. When the mole fraction of 4-ATP is below 0.3, 4-ATP molecules have a stronger tendency to adsorb on a gold surface than EG_4-SH. Above 0.3, the difference in the adsorption tendencies between the thiols decreases.

For any mixed SAM monolayer containing 4-ATP, capacitance measurements are not suitable for use in characterizing the surface composition of the mixed monolayer. One reason could be that the defects in this SAM monolayer can no longer be ignored as they have a significant effect on the capacitance of the SAM. The other reason could be that 4-ATP is an electroactive compound. Electrons can reach the gold surface from the electrolyte solution and thus increase the capacitance values of SAM monolayer containing 4-ATP.

4.2 Quantification of nonspecific adsorption on mixed SAM biosensor platforms using electrochemical enzyme immunoassay. By using electrochemical enzyme immunosensors, protein adsorption on mixed SAMs of decanethiol and oligo(ethylene glycol) was determined. On the OEG-SAM surface, the protein adsorption was reduced considerably more than on the hydrophobic decanethiol SAM surface. The OEG-SAM surface thus offers a better non-fouling surface than a DT-SAM surface. Quantifying the nonspecific adsorption on mixed SAM monolayer of DT and EG_4-SH, revealed that mixed SAM surfaces modified with mole fractions of EG_4-SH more than

0.2 have an adequate ability to resist nonspecific adsorption on the electrochemical enzyme immunosensors.

For electrochemical immuno-sandwich biosensor platforms with mixed SAMs of template species of 4-ATP and blocking species of DT or EG_4-SH, resistance of alkanethiol and oligo(ethylene glycol) to nonspecific adsorption was compared. In order to analyze the nonspecific adsorption on immuno-sandwich biosensor platforms, the amount of specific adsorption on mixed SAM monolayers was first studied by determining the amount of polyaniline electrodeposited on mixed SAM-modified Au electrodes with various mole fractions of 4-aminothiophenol in the SAMs. The results revealed that for the same mole fraction of 4-ATP in the SAM, the amount of polyaniline film deposited on 4-ATP/EG_4-SH mixed monolayers was the same as that grown on 4-ATP/DT mixed SAM monolayers. Consequently, the amount of specific adsorption on these two mixed SAM systems with the same mole fraction of 4-ATP in the SAM can be considered to be the same, allowing the quantification of the nonspecific adsorption on immuno-sandwich biosensor platforms. For conditions of the same mole fraction of 4-ATP in mixed SAM monolayers, distinctly lower protein adsorption occurs on surfaces with EG_4-SH/4-ATP than on DT/4-ATP SAM surfaces. EG_4-SH monolayers therefore offer better inhibition to nonspecific adsorption than DT monolayers. When the mole fraction of EG_4-SH in the mixed SAM is more than 0.85 an EG_4-SH/4-ATP monolayer is good enough to reduce nonspecific adsorption, but when the mole fraction of EG_4-SH in the SAM exceeds 0.85, less polyaniline thin films will be electrodeposited on the EG_4-SH/4-ATP monolayer as there is less 4-ATP in the SAM. This result shows that in real electrochemical immuno-sandwich biosensor devices, an EG_4-SH monolayer does not

increase its ability to resist nonspecific adsorption noticeably more than in a DT monolayer because the electrochemical signal due to nonspecific adsorption is small compared to the electrochemical signal due to specific adsorption on a mixed SAM monolayer.